27 September 2019

HCMV glycoprotein B nucleoside-modified mRNA vaccine elicits antibody responses with greater durability and breadth than MF59-adjuvanted gB protein immunization

Short Title: Immunogenicity of next-generation HCMV gB vaccines

Cody S. Nelson[1]*, Jennifer A. Jenks[1], Norbert Pardi[2], Matthew Goodwin[1], Hunter Roark[1], Whitney Edwards[3], Jason S. McLellan[4], Justin Pollara[3], Drew Weissman[2], Sallie R. Permar[1]

[1]Human Vaccine Institute, Duke University Medical Center, Durham, NC, USA.

[2]Department of Medicine, University of Pennsylvania Perelman School of Medicine, Philadelphia, PA, USA.

[3]Department of Surgery, Duke University Medical Center, Durham, NC, USA.

[4]Department of Molecular Biosciences, University of Texas at Austin, Austin, TX, USA.

* Please address correspondence to Cody S. Nelson (cody.nelson@duke.edu)

Keywords: cytomegalovirus, vaccines, glycoprotein B

Abstract WC: 300 (300 max)

Author summary WC: 188 (200 max)

Main Text WC: 3,177

Methods WC: 3,142

Abstract:

A vaccine to prevent maternal acquisition of human cytomegalovirus (HCMV) during pregnancy is a primary strategy to reduce the incidence of congenital disease. Similarly, vaccination of transplant recipients against HCMV has been proposed to prevent transplant-associated HCMV morbidity. The MF59-adjuvanted glycoprotein B protein subunit vaccine (gB/MF59) is the most efficacious tested to-date for both indications. We previously identified that gB/MF59 vaccination elicited poor neutralizing antibody responses and an immunodominant response against gB antigenic domain 3 (AD-3). Thus, we sought to test novel gB vaccines to improve functional antibody responses and reduce AD-3 immunodominance. Groups of juvenile New Zealand White rabbits were administered 3 sequential doses of full-length gB protein with an MF59-like squalene adjuvant (analogous to clinically-tested vaccine), gB ectodomain protein (lacking AD-3) with squalene adjuvant, or lipid nanoparticle (LNP)-packaged nucleoside-modified mRNA encoding full-length gB. The AD-3 immunodominant IgG response following human gB/MF59 vaccination was closely mimicked in rabbits, with 78% of binding antibodies directed against this region in the full-length gB protein group compared to 1% and 46% in the ectodomain and mRNA-LNP-vaccinated groups, respectively. All vaccines were highly immunogenic with similar kinetics and comparable peak gB-binding and functional antibody responses. Although gB ectodomain subunit vaccination reduced targeting of non-neutralizing epitope AD-3, it did not improve vaccine-elicited neutralizing or non-neutralizing antibody functions. gB nucleoside-modified mRNA-LNP-immunized rabbits exhibited enhanced durability of IgG binding to soluble and cell membrane-associated gB protein as well as HCMV-neutralizing function. Furthermore, the gB mRNA-LNP vaccine enhanced breadth of IgG binding responses against discrete gB peptide residues. Finally, low-magnitude gB-specific T cell activity was observed in the full-length gB protein and mRNA-LNP vaccine groups, though not in ectodomain-vaccinated rabbits. Altogether, these data suggest that the gB mRNA-LNP vaccine candidate, aiming to improve upon the partial efficacy of gB/MF59 vaccination, should be further evaluated in preclinical models.

53 **Author summary:**

54 Human cytomegalovirus (HCMV) is the most common infectious cause of infant birth defects,
55 resulting in permanent neurologic disability for one newborn child every hour in the United States.
56 Furthermore, this virus causes significant morbidity and mortality in immune-suppressed
57 transplant recipients. After more than a half century of research and development, we remain
58 without a clinically-licensed vaccine or therapeutic to reduce the burden of HCMV-associated
59 disease. In this study, we sought to improve upon the glycoprotein B protein vaccine (gB/MF59),
60 the most efficacious HCMV vaccine evaluated in clinical trial, via targeted modifications to either
61 the protein structure or vaccine formulation. An attempt to alter the protein structure to focus the
62 immune response on vulnerable epitopes ('gB ectodomain') had little effect on the quality or
63 function of the vaccine-elicited antibodies. However, a novel vaccine platform, nucleoside-
64 modified mRNA formulated in lipid nanoparticles, increased the durability and breadth of vaccine-
65 elicited immune responses. We propose that an mRNA-based gB vaccine may ultimately prove
66 more efficacious than the gB/MF59 vaccine and should be further evaluated for its ability to elicit
67 antiviral immune factors that can prevent both infant and transplant-associated disease caused
68 by HCMV infection.

Introduction:

Human cytomegalovirus (HCMV) impacts 1 in 150 live born infants, making this pathogen the most common cause of congenital infection worldwide [1, 2]. Approximately 20% of infants infected with HCMV *in utero* will develop long-term sequelae including microcephaly, intrauterine growth restriction, hearing/vision loss, or neurodevelopmental delay [3, 4]. Furthermore, HCMV is the most prevalent infection among solid organ and hematopoietic stem cell transplant recipients, causing end-organ disease such as gastroenteritis, pneumonitis, or hepatitis and potentially predisposing these individuals to allograft rejection and/or failure [5, 6]. However, we remain without a vaccine or immunotherapeutic intervention to reduce the burden of disease among newborn children and transplant recipients.

A variety of vaccine platforms and formulations have been trialed for the prevention of both congenital (reviewed in [7]) and transplant-associated HCMV disease (reviewed in [8]), of which the most efficacious has been the glycoprotein B (gB) subunit vaccine administered with MF59 squalene adjuvant [9]. gB is the viral fusogen and is essential for entry into all cell types [10], including placental trophoblast progenitor cells [11]. Furthermore, gB is highly-expressed and an immune-dominant target following natural infection, making this protein an attractive target for vaccination. gB/MF59 subunit vaccination demonstrated moderate (~50%) efficacy in blocking HCMV infection and host seroconversion in populations of HCMV-seronegative postpartum [12] and adolescent women [13]. Furthermore, in transplant recipients this vaccine protected against HCMV viremia and reduced the clinical need for antiviral treatment [14].

Analysis of samples obtained from both postpartum and transplant-recipient gB vaccinees revealed two key observations regarding the target and function of gB-elicited antibody responses that inform our understanding of the partial vaccine efficacy. First, we identified that vaccination elicited an extraordinarily robust response against antigenic domain 3 (AD-3), a cytosolic non-neutralizing epitope in the C-terminal region of the protein [15]. Second, we noted that gB-specific antibodies elicited in postpartum women and transplant-recipients were predominantly non-

neutralizing, suggesting that the mechanism of partial protection against viral acquisition was not the induction of neutralizing antibodies [15, 16]. However, the protective non-neutralizing function remains unclear: we identified that gB/MF59 vaccinees had high-magnitude viral phagocytosis activity, though magnitude was not associated with infection status [15]. These results led us to hypothesize that we might improve upon the gB/MF59 vaccine through rational design of novel immunogens that minimize responses against the intracellular to gB AD-3 epitope.

Here we present an investigation into the immunogenicity of two novel gB vaccines aiming to reduce exposure to AD-3: a truncated gB protein subunit vaccine (lacking the AD-3 epitope) administered with MF59-like squalene adjuvant AddaVax (gB ectodomain vaccine) and a gB nucleoside-modified mRNA vaccine packaged in lipid nanoparticles (gB mRNA-LNP vaccine). New Zealand White rabbits were selected for this study because we previously identified that neutralizing and non-neutralizing antibodies are elicited in rabbits by vaccination, and that F_c receptor-independent and dependent effector functions can be measured *in vitro* [17]. Three groups of rabbits were vaccinated with either: 1) full-length gB + AddaVax (immunogen from gB/MF59 vaccine trial; ‘gB FL’), 2) gB ectodomain + AddaVax (‘gB ecto’), or 3) gB mRNA-LNP (‘gB mRNA). We anticipated that gB ectodomain and gB mRNA-LNP vaccines would have reduced targeting of AD-3 and enhanced neutralizing and/or non-neutralizing function, resulting in a superior vaccine that might be deployed to prevent both congenital and transplant-associated HCMV disease.

Results:

IgG binding to soluble and cell-associated gB

We first assessed the ability of IgG elicited by all three vaccines (**Figure 1;** gB FL, gB ecto, and gB mRNA) to bind soluble full-length gB (**Figure 2A**) and gB ectodomain proteins (**Figure 2B**) by BAMA, as well as cell-associated gB on the surface of gB-transfected cells by flow cytometry (**Figure 2C**). All vaccines were highly immunogenic, with similar peak immunogenicity (10 weeks) binding magnitude to both soluble and cell-associated gB. However, gB mRNA-immunized rabbits had enhanced binding to both soluble and cell-associated gB at the time of animal necropsy (20 weeks), indicating superior durability of the mRNA vaccine-elicited antibody responses compared to gB FL. This distinction was most pronounced for binding to cell-associated gB (median % PE+ cells at 20 weeks: mRNA = 29.1% vs FL = 18.8%, p=0.01, Kruskal-Wallis + *post hoc* Mann-Whitney U test). Additionally, we evaluated the avidity of vaccine-elicited IgG responses by plate-based, urea wash ELISA (**Figure 2D**). We noted slightly reduced median RAI (relative avidity index, measured against soluble gB FL protein) in gB mRNA-immunized rabbits, though the difference was not statistically significant.

Linear gB epitope binding

To identify the epitope specificity and breadth of IgG responses elicited by each vaccine, we utilized a peptide microarray library consisting of 15-mers overlapping each subsequent peptide by 10 residues and spanning the entire gB ORF (Towne strain) (**Figure 3A**). We observed that rabbits administered the gB FL vaccine had a nearly identical AD-3 epitope immunodominance to that observed in human gB/MF59 vaccinees [18], with 77% of the peptide-binding IgG response directed against this singular region (vs. 78% in human vaccinees). AD-3 linear peptide binding was dramatically reduced in gB ecto (<1%) and gB mRNA (46%) groups. However, AD-3 remained the dominant response in gB FL and gB mRNA groups, while the furin cleavage site was dominant for gB ecto (no AD-3 in the immunogen) (**Figure S1**). Furthermore,

gB mRNA vaccinated rabbits had slightly reduced total peptide binding compared to gB FL (**Figure 3B**; median peptide-binding MFI sum: FL = 96,629, mRNA = 48,051, p=ns, Kruskal-Wallis + *post hoc* Mann-Whitney U test), though both gB FL and gB mRNA had greater total peptide binding than the gB ecto group (both $p<0.05$, Kruskal-Wallis + *post hoc* Mann-Whitney U test). Importantly, there was enhanced breadth of peptide-binding responses in gB mRNA vaccinated rabbits compared to both gB FL and gB ecto groups (**Figure 3D**; median number of discrete peptides bound: FL = 44.5, ecto = 28.5, mRNA = 85, both $p<0.05$, Kruskal-Wallis + *post hoc* Mann-Whitney U test). Of note, the pattern of linear peptide binding and breadth of mRNA-immunized rabbits appears analogous to that elicited by natural HCMV infection [18].

Vaccine-elicited IgG binding to neutralizing epitopes and HCMV neutralization

We next examined IgG binding to regions of gB known to be targeted by neutralizing antibodies Domain 1 (AD-4), Domain 1+2 (AD-4 + AD-5), AD-1, and AD-2 (**Figure 4A-D**). Notably, we did not identify vaccine-elicited antibodies against AD-2 in any of the 3 vaccine groups (**Figure 4D**), an epitope known to be the target of potently-neutralizing gB-specific antibodies associated with reduced viremia in transplant recipients [19] and protection against congenital transmission [20]. Furthermore, low responses were noted against AD-1 (**Figure 4C**). The kinetics of vaccine-elicited IgG binding against Domain 1 as well as Domain 1+2 mirrored those of binding to soluble gB protein (**Figure 2**), However, at 20 weeks both gB ecto and gB mRNA vaccinated rabbits had enhanced binding against Domain 1 compared to gB FL (median Domain 1 MFI at 20 weeks: FL = 571, ecto = 2,343, mRNA = 2,730, $p<0.05$ for both, Kruskal-Wallis + *post hoc* Mann-Whitney U test) (**Figure 4A**).

Furthermore, we assessed the magnitude of vaccine-elicited HCMV neutralization against heterologous (cross strain) AD169-revertant virus in fibroblast and epithelial cell lines, both in the presence and absence of purified rabbit complement (**Figure 4E-H**). Neutralization was enhanced in the presence of complement (**Figure 4G,H**) as previously noted [18]. All three vaccines had

166 similar peak neutralization at 10 weeks (median AD169r ID_{50} in fibroblast at 10 weeks +C: FL =
167 158, ecto = 184, mRNA = 174). gB mRNA vaccinated rabbits had two-fold higher virus
168 neutralization at 20 weeks, indicating superior response durability, though this distinction was not
169 statistically significant (median AD169r ID_{50} in fibroblast at 20 weeks +C: FL = 49, ecto = 62,
170 mRNA = 120, p=0.12, Kruskal-Wallis + *post hoc* Mann-Whitney U test). Notably, neutralizing
171 responses measured in both fibroblast and epithelial cells were similar in magnitude, as might be
172 expected for gB-specific antibodies. In addition to heterologous AD169r, we also measured
173 neutralization of autologous (vaccine strain) Towne virus in fibroblast cells (**Figure S2A,B**), but
174 identified little difference between vaccination groups.
175
176 *Vaccine-elicited engagement of $F_c\gamma$ receptors and non-neutralizing effector functions*
177 We next investigated the ability of vaccine-elicited antibodies to engage $F_c\gamma$ receptors
178 (specifically $F_c\gamma$RI, $F_c\gamma$RIIa, $F_c\gamma$RIIb, and $F_c\gamma$RIIIa) which is a prerequisite for F_c-mediated effector
179 functions (**Figure 5A-D**). Intriguingly, a single dose of gB mRNA vaccine (but not gB FL or gB
180 ecto) resulted in the rapid development of antigen-specific IgG that could engage with F_c receptors
181 (**Figure S3**), which might be due to robust induction of T follicular helper cells that facilitate B cell
182 maturation and class switching [21]. This distinction was most notable for $F_c\gamma$RIIa and $F_c\gamma$RIIb (2
183 weeks median $F_c\gamma$RIIa MFI: FL = 0 vs. mRNA = 128, p=0.02, Kruskal-Wallis + *post hoc* Mann-
184 Whitney U test). At peak immunogenicity (10 weeks), gB-specific antibody engagement of $F_c\gamma$
185 receptors was similar between vaccine groups. However, at the time of necropsy we generally
186 noted enhanced median binding to $F_c\gamma$R's among gB mRNA-vaccinated rabbits vs. gB FL, though
187 this comparison was only significant for $F_c\gamma$RIIIa (20 weeks median $F_c\gamma$RIIIa MFI: FL = 3,929 vs.
188 mRNA = 10,933, p=0.02, Kruskal-Wallis + *post hoc* Mann-Whitney U test).
189 We next investigated the magnitude of non-neutralizing, F_c effector functions mediated by
190 vaccine-elicited antibodies. First, we measured antibody-dependent cellular phagocytosis
191 (ADCP) of whole HCMV virions (TB40/E strain) (**Figure 5E**). We identified similar peak

192 phagocytosis activity (10 weeks), but intriguingly we noted enhanced phagocytosis in gB FL
193 vaccinees at 20 weeks indicating more robust phagocytosis durability in this group (median
194 %phagocytosing cells: FL = 10.1% vs. mRNA = 7.1%, p<0.01, Kruskal-Wallis + *post hoc* Mann-
195 Whitney U test). Next, we assessed NK cell degranulation activity (CD107a upregulation) when
196 vaccine-elicited antibodies are incubated with HCMV-infected cells (**Figure 5F**), which we
197 previously identified to approximate antibody-dependent cellular cytotoxicity (ADCC) for rabbits
198 [17]. However, we were unable to measure NK degranulation activity for the majority of animals,
199 suggesting that antibodies mediating this non-neutralizing effector function are not a dominant
200 response elicited by gB FL, gB ecto, or gB mRNA vaccines.
201
202 *gB non-ectodomain-directed antibodies can mediate whole HCMV virion phagocytosis*
203 We depleted gB ectodomain-specific IgG from vaccinated rabbit sera, and depletion was
204 confirmed by ELISA against the same protein (**Figure 6A**). Furthermore, we established that AD-
205 3-specific antibodies remained in gB ectodomain-depleted sera of gB FL vaccinees by measuring
206 responses to an immunodominant AD-3 peptide (**Figure 6B).** Interestingly, ectodomain-depleted
207 rabbit sera was able to mediate low-level HCMV virion phagocytosis (**Figure 6C**) (gB FL median
208 % phagocytosing cells: preimmune = 0.96%, mock depleted = 2.91%, gB ecto depleted = 1.93%),
209 suggesting that non-ectodomain epitopes (e.g. AD-3 or MPER) can be bound by circulating IgG
210 that can subsequently mediate non-neutralizing effector functions. Furthermore, the magnitude of
211 vaccine-elicited binding to AD-3 linear peptides of non-depleted plasma correlated strongly with
212 phagocytosis mediated by gB ectodomain-depleted serum antibodies (**Figure 6D**; r = 0.75,
213 p<0.001, Spearman-rank correlation).
214
215 *gB-specific T cell responses*
216 Lastly, we investigated the magnitude of antigen-specific T cells by intracellular cytokine
217 staining. Purified spleen mononuclear cells were either not stimulated, incubated with mitogen

concanavalin A (ConA), or incubated with pooled gB peptides. Subsequently, the concentration of IFNγ$^+$ live T cells identified for each group/treatment (**Figure 7A**). For animals from each vaccine group, ConA nonspecifically stimulated a population of T cells to produce IFNγ$^+$ (all $p<0.05$, Friedman test + *post hoc* Wilcoxon matched pairs signed-rank test). When the percentage of unstimulated IFNγ$^+$ T cells is subtracted from that of gB-stimulated IFNγ$^+$ T cells (**Figure 7B**), we observed a modest gB-specific T cell response that is most pronounced in gB FL and gB mRNA vaccinated rabbits (median % gB-specific IFNγ$^+$ T cells: FL = 0.22%, ecto = 0%, mRNA = 0.38%, p=ns, Kruskal-Wallis). In addition to spleen cells, we attempted to identify antigen-specific T cells in peripheral blood as well as mesenteric lymph nodes, but no IFNγ$^+$ cells were observed using this method upon either ConA or gB peptide stimulation.

Discussion:

Glycoprotein B, a homotrimeric viral fusogen that is essential for entry into all cell types, has long been a leading HCMV vaccine candidate [9]. Yet over the past decade, following discovery that the most potent HCMV-neutralizing antibodies in human sera target the gH/gL/UL128-131A pentameric complex [22, 23], the focus has expanded from gB vaccine development. Nevertheless, it is important to recognize that the gB/MF59 protein subunit vaccine achieved partial moderate vaccine efficacy in preventing primary HCMV infection and seroconversion [12, 13] – a feat unparalleled in the HCMV vaccine field [24]. Furthermore, the gB/MF59 vaccine reduced viremia and demonstrated a protective benefit in transplant recipients [14]. Importantly, these partial successes were achieved without the elicitation of robust neutralizing antibody responses [16, 25]. In this investigation we sought to improve upon the gB immunogen antigenicity and vaccine/delivery platform, comparing novel vaccine immunogenicity head-to-head against the gB/MF59 vaccine in a preclinical model.

HCMV preclinical vaccine development is hindered by the fact that small animal models poorly represent host-pathogen biology and mechanisms of disease pathogenesis [26, 27]. We chose to test immunogenicity in rabbits because we previously demonstrated that vaccination can elicit antibodies with both neutralizing and non-neutralizing *in vitro* functionality [17]. In this study we were able to epitope-map and define the function of antibodies elicited by these three experimental vaccines, then compare to previously-reported immune correlates of protection (Nelson, *Journal of Infectious Diseases*, 2019, in press). HCMV-neutralizing IgG has previously been associated with reduced viral systemic dissemination [20, 28, 29]. Specifically, antibodies targeting gB AD-2 are correlated with reduced incidence of viremia and congenital disease [19, 20], though AD-2-specific antibodies were not elicited to any appreciable extent by the vaccines tested in this investigation (**Figure 4H**). Furthermore, non-neutralizing antibodies targeting gB and other surface glycoproteins are well described to have a protective role in preventing HCMV acquisition [16, 25], reducing viremia [16, 30], and blocking tissue-invasive replication [30, 31],

254 though the precise mechanism remains unknown. Lastly, HCMV-specific $CD4^+$ and $CD8^+$ T cells
255 have been widely implicated in reducing HCMV acquisition [32, 33], viral replication [26, 34-42],
256 and the incidence of congenital/transplant-associated disease [43, 44].

257 Given the uncertainty regarding precise epitope specificities or immune effector functions
258 protective against HCMV-associated disease, we regarded enhanced *durability* and *breadth* of
259 immune responses as desirable attributes for vaccine development and the primary outcomes of
260 interest in this study. Overall, we identified that the experimental vaccines (gB FL, gB ecto, and
261 gB mRNA) elicited comparable magnitude binding and functional antibody responses at peak
262 immunogenicity. Most distinction between vaccine-elicited immunogenicity was observed only at
263 the latest timepoint (20 weeks – 12 weeks after final vaccine dose), signifying variable durability
264 of elicited antibody responses. Nucleoside-modified mRNA-LNP vaccines have been well-
265 described to produce sustained antigen presentation with robust T follicular helper cell and
266 germinal center B cell stimulation, resulting in extraordinarily durable antibody responses after
267 even a single vaccine dose in small and large animals [21, 45-47]. Indeed, we identified that the
268 durability of gB mRNA vaccine-elicited responses exceeded that of gB FL for nearly all measured
269 antibody binding/functional responses (**Table 1**; comparison statistically significant for: soluble
270 and cell-associated gB binding, binding to gB domain 1 and domain 1+2, heterologous virus
271 neutralization, and engagement of $F_c\gamma$RIIIa). Furthermore, we noted enhanced breadth of the
272 peptide-binding immune response in gB mRNA-immunized rabbits, resulting in the targeting of
273 unconventional/sub-dominant epitopes that are not observed in protein subunit vaccinees (**Figure**
274 **3, Figure S1**). mRNA-vaccinated rabbits appear to have a gB peptide-binding fingerprint that
275 closely resembles that in seropositive individuals elicited by natural host infection [25].
276 Importantly, while HCMV gB mRNA vaccines have been tested previously in a preclinical model
277 [48], this is the first such investigation to test a gB mRNA-based vaccine alongside the partially-
278 effective gB/MF59 protein subunit vaccination and to directly compare the epitope specificity,

279 durability, and neutralizing/non-neutralizing function of antibodies elicited by these two vaccine
280 platforms.

281 In this investigation, we specifically focused on the implications of the gB/MF59-elicited
282 immune-dominant response directed against gB AD-3 [25]. We hypothesized the absence of
283 neutralizing antibodies in gB/MF59 vaccinees may be attributable to the dominant responses
284 against the AD-3 'decoy epitope', which diverted antibody targeting away from 'more functional'
285 epitopes [24]. We directly tested this hypothesis with our gB ecto group by excluding AD-3 from
286 the immunogen. Intriguingly, we failed to see any consistent increase in the magnitude of
287 functional neutralizing/non-neutralizing antibodies in gB ecto vaccinated rabbits, suggesting that
288 inclusion of the AD-3 epitope in the vaccine immunogen does not hinder the development of more
289 functional antibodies. Is it therefore possible that AD-3 directed antibodies have any functional or
290 protective role that might account for the 50% vaccine efficacy observed in gB/MF59 vaccinees?
291 In this study we noted that AD-3-specific antibodies can mediate non-neutralizing antibody
292 effector functions including whole virion phagocytosis (**Figure 6**). Consequently, the high-
293 magnitude AD-3 response in gB FL-vaccinated rabbits likely accounts for our observation of
294 robust and durable phagocytosis activity in these animals (**Figure 5E**).

295 A limitation to this study is dissimilarity in vaccine dose and route of delivery between
296 comparison groups. Protein subunit vaccines (gB FL, gB ecto) were given I.M. at a dose of 20μg,
297 mimicking the protocol for gB/MF59 immunized humans in the partially-efficacious clinical trials
298 [12, 13, 24]. In contrast, 50μg of the gB nucleoside-modified mRNA-LNP was administered I.D,
299 which was selected because this delivery method enhances protein expression *in vivo* [49].
300 Depending on the antigen and vaccine formulation, intradermal vaccination may be as much as
301 10 times more potent than intramuscular dosing [50]. Therefore, we cannot rule out the possibility
302 that our results of enhanced breadth and durability in gB mRNA-immunized rabbits are
303 dose/method dependent – that a higher dose or different delivery method of gB FL protein might
304 not have achieved similar results to gB mRNA-LNP vaccinated rabbits. Furthermore, while rabbits

provide an excellent model to study vaccine immunogenicity, this investigation was restricted by the rabbit immunologic toolbox. We were able to measure $F_c\gamma$ receptor engagement in this study, though lacked the ability to identify the mechanism behind variable $F_c\gamma$ receptor engagement (e.g. IgG subclass or F_c glycosylation). Furthermore, while we were able to identify gB-specific T cells in spleen, we were unable to: 1) identify antigen-specific T cells in peripheral blood, and 2) parse out T cell subsets ($CD4^+$, $CD8^+$, etc). Nevertheless, the results described are sufficient justification for subsequent testing of the gB mRNA-LNP vaccine in nonhuman primate preclinical challenge models and/or human clinical trials.

This comparison of immune responses elicited by next-generation HCMV vaccines, head-to-head against gB/MF59 immunization (gB FL), provides a basis for rational gB vaccine development efforts. First, we have demonstrated that gB nucleoside-modified mRNA-LNP immunization improves the durability of gB-binding and functional antibody responses and enhances the breadth of the gB-specific antibody repertoire. Additionally, we note that gB ectodomain immunization did not elicit antibody responses that were functionally superior to gB FL, suggesting that the immunodominant AD-3 response does not interfere with the development of functional antibodies. While we await well-validated immune correlates of protection to inform HCMV vaccine development efforts, the gB mRNA-LNP vaccine clearly had enhanced long-term immunogenicity and response breadth compared with gB FL and gB ecto vaccines. Therefore, we propose subsequent testing of this vaccine platform in nonhuman primate challenge models as well as human immunogenicity trials to rigorously interrogate its ability to elicit immune factors protective against congenital HCMV infection and transplant-associated disease.

Methods:

gB ectodomain immunogen production. The sequence encoding the ectodomain segment (amino acid residues 1-696) of Towne strain (GenBank accessioning# FJ616285.1) HCMV glycoprotein B (gB) was tagged at the 3' end with a polyhistidine tag, and the furin cleavage site at residue 457 mutated from 'RTKR' to 'STKS'. The nucleotide sequence was codon-optimized for mammalian cells, then cloned into pcDNA3.1(+) mammalian expression vector (Invitrogen) via *BamHI* site at the 5' end and *EcoRI* site at the 3' end. Subsequently, the plasmid was transiently transfected into Expi293i cells using ExpiFectamine 293 transfection reagents (ThermoFisher Scientific) according to the manufacturer's instructions. Culture supernatant was harvested after 5 days of incubation at 37 °C and 8% CO_2, then purified using Nickel-NTA resin (ThermoFisher Scientific). Purity, identity, and correct molecular weight were confirmed by Western blot using monoclonal antibodies specific for gB AD-2, gB domain 1, and gB domain 2 (described in [15]), followed AP-conjugated anti-human IgG (Sigma-Aldrich). Finally, the protein was tested for the presence of endotoxin using the Pierce LAL chromogenic endotoxin quantitation kit (ThermoFisher Scientific). gB protein ectodomain aliquots were stored at -80°C at a concentration of ~1 μg/μl, then thawed <60 minutes prior to injection.

gB mRNA production and formulation into lipid nanoparticles. The modified mRNA encoding HCMV gB (Towne strain, GenBank accessioning# FJ616285.1) was produced as previously described [51] using T7 RNA polymerase (Megascript, Ambion) on codon-optimized [52] linearized plasmid (sequence is available upon request). The mRNA was transcribed to contain 101 nucleotide-long poly(A) tail. To generate modified nucleoside-containing mRNA, m1Ψ-5′-triphosphate (TriLink) was used instead of UTP. The mRNA was then capped using the m7G capping kit with 2′-*O*-methyltransferase (ScriptCap, CellScript). The mRNA was purified by Fast Protein Liquid Chromatography (FPLC) (Akta Purifier, GE Healthcare), as described [53] and analyzed by electrophoresis using denaturing or native agarose gels, and stored at −20 °C. The

352 FPLC-purified m1Ψ-containing HCMV gB mRNA and poly(C) RNA (Sigma) were encapsulated in
353 LNPs using a self-assembly process in which an aqueous solution of mRNA at pH=4.0 is rapidly
354 mixed with a solution of lipids dissolved in ethanol [54]. LNPs used in this study were similar in
355 composition to those described previously [54, 55], which contain an ionizable cationic lipid
356 (proprietary to Acuitas)/phosphatidylcholine/cholesterol/PEG-lipid (50:10:38.5:1.5 mol/mol) and
357 were encapsulated at an RNA to total lipid ratio of ~0.05 (wt/wt). They had a diameter of ~80 nm
358 as measured by dynamic light scattering using a Zetasizer Nano ZS (Malvern Instruments Ltd)
359 instrument. mRNA-LNP formulations were stored at -80°C at a concentration of mRNA of ~1 μg/μl,
360 then thawed <60 minutes prior to injection.
361
362 *Animal care and sample collection*. Juvenile New Zealand White rabbits (approximately 10 weeks
363 of age), were purchased from Robinson Services Inc (Mocksville, NC) and housed at Duke
364 University. For blood collections, animals were sedated with 1mg/kg subcutaneous acepromazine
365 and topical 1% lidocaine applied to the ears. EDTA-anticoagulated blood was collected via
366 auricular venipuncture. Plasma was separated from whole blood by centrifugation, and PBMCs
367 were isolated by density gradient centrifugation using Lympholyte cell separation media
368 (Cedarlane laboratories). Animals were euthanized using 0.5mL of subcutaneously-injected
369 xylazine (100mg/mL) + ketamine (500mg/mL) mixed together in a 1:5 ratio, followed by 0.5mL of
370 intracardiac Euthasol (pentobarbital sodium + phenytoin sodium). Lymphocytes were isolated
371 from spleen and mesenteric lymph nodes by manual tissue disruption and crushing through a
372 100μm cell strainer, followed by density gradient centrifugation with Lympholyte cell separation
373 media.
374
375 *Animal vaccination.* Three groups of juvenile New Zealand White rabbits (n=6) were given
376 different vaccines: 1) 50μg intramuscular full-length gB protein (generous gift of Sanofi Pasteur)
377 combined 1:1 v/v with MF59-like squalene adjuvant AddaVax (Invivogen), 2) 50μg intramuscular

gB ectodomain protein combined 1:1 v/v with AddaVax, or 3) 50µg intradermal nucleoside-modified gB mRNA packaged in lipid nanoparticles. Vaccine doses were administered monthly for three consecutive months. For intramuscular (I.M.) protein subunit vaccine administration, rabbits were sedated with 1mg/kg subcutaneous acepromazine then injected with the vaccine dose in the rear thigh (alternating sides between monthly doses). For intradermal (I.D.) mRNA-LNP vaccine administration, rabbits were sedated with 1mg/kg subcutaneous acepromazine as well as 2% inhaled isofluorane, and the saddle of the rabbit shaved. Chilled, sterile PBS was added to each vaccine dose to a total volume of 300 µL, the diluted vaccine divided into 6 equal fractions of 50µL each, then the rabbit saddle was injected intradermally with 3 injections on each side of the spine (injection sites varied between monthly doses).

Cell culture. Human retinal pigment epithelial (ARPE-19) cells (ATCC) were maintained for a maximum of 35 passages in Dulbecco's modified Eagle medium-12 (DMEM-F12) supplemented with 10% FCS, 2mM L-glutamine, 1mM sodium pyruvate, 50 U/mL penicillin, 50 µg/mL streptomycin and gentamicin, and 1% epithelial growth cell supplement (ScienCell). Human lung (MRC-5) fibroblasts (ATCC) were maintained for a maximum of 20 passages in DMEM containing 20% FCS, 50 U/mL penicillin, and 50 µg/mL streptomycin. Human epithelial kidney (HEK293T) cells (ATCC) were maintained for a maximum of 35 passages in DMEM containing 10% FCS, 25mM HEPES buffer, 50 U/mL penicillin, and 50 µg/mL streptomycin. Human monocyte (THP-1) cells (ATCC) were maintained for a maximum of 35 passages in RPMI-1640 medium containing 10% FCS. All cell lines were tested for the presence of mycoplasma biannually.

Virus growth. AD169 revertant virus (AD169r; a gift from Merck) [56], and BADUL131a virus [57] stocks were propagated on ARPE cells in T75 culture flasks. Towne virus (ATCC) was propagated on MRC-5 cells in T75 culture flasks. Supernatant containing cell-free virus was collected when 90% of cells showed cytopathic effects, then cleared of cell debris by low-speed

404 centrifugation before passage through a 0.45-µm filter. Viral infections of ARPE-19 cells were
405 carried out in similar media but contained only 5% FCS and lacking cell growth supplement.
406
407 *Binding antibody multiplex assay (BAMA).* Antibody responses against gB full-length protein, gB
408 ectodomain, and gB epitopes (creation described in [14, 20]) were assessed by multiplex ELISA.
409 In brief, carboxylated fluorescent beads (Luminex) were covalently coupled to purified HCMV
410 antigens and subsequently incubated with maternal plasma in assay diluent (phosphate-buffered
411 saline, 5% normal goat serum, 0.05% Tween 20, and 1% Blotto milk, 0.5% polyvinyl alcohol, and
412 0.8% polyvinylpyrrolidone). The antigen panel included full-length gB (courtesy of Sanofi-
413 Pasteur), gB ectodomain protein, gB domain 1, gB domain 2, gB domain 1+2, gB AD-1
414 (myBiosource), and biotinylated linear gB AD-2 (biotin-NETIYNTTLKYGD). HCMV glycoprotein–
415 specific antibodies were detected with phycoerythrin-conjugated goat anti-human IgG (2 µg/mL,
416 Southern Biotech). Beads were washed and acquired on a Bio-Plex 200 instrument (Bio-Rad),
417 and results were expressed as mean fluorescence intensity. A panel of pre-vaccination time
418 points was tested to determine nonspecific baseline levels of binding. Minimal background activity
419 was observed, so the threshold for positivity for each antigen was set at the mean value of
420 negative control sera to each antigen + 3 standard deviations. Blank beads were used in all
421 assays to account for nonspecific binding. All assays included tracking of HCMV immunoglobulin
422 (Cytogam – CSL Behring) standard by Levy-Jennings charts. The preset assay criteria for sample
423 reporting were coefficient of variation per duplicate values of ≤20% for each sample and ≥100
424 beads counted per sample. All samples were analyzed at the same dilution for each antigen: full-
425 length gB, gB ectodomain, gB domain 1, gB domain 2, and gB domain 1+2 were assessed at a
426 1:500 dilution; gB AD-1 and gB AD-2 were assessed at a 1:50 dilution. These dilutions were
427 predetermined to be within the linear range of the assay based on testing serial dilutions of a
428 small subset of plasma samples.
429

F_cγ receptor engagement. The binding of vaccine-elicited serum antibodies to F_cγ receptors was characterized using a multiplex F_cγ receptor BAMA assay, employing the reagents and QC methods described above. In brief, HCMV gB (full-length) was covalently coupled to streptavidin (Rockland)-coupled fluorescent beads (Luminex). Sera samples were diluted 1:500, then incubated in duplicate in a 96-well microplate with gB-streptavidin-coupled beads, then washed and incubated with one of the following biotinylated F_cγ receptor tetramers: F_cγRIa, F_cγRIIa (clone H131), F_cγRIIb, and F_cγRIIIa (clone V158) (F_cγ receptor proteins courtesy of Dr. Kevin Saunders). F_cγ receptor engagement was detected using mouse anti-human IgG-PE (myBioSource) followed by a final wash. Data were acquired on a BioPlex-200 (Luminex).

gB-transfected cell binding. Binding of vaccine-elicited antibodies to trimeric gB expressed on cell membranes was assessed by flow cytometry as previously [15]. Briefly, HEK293T cells were grown overnight to ~50% confluency, then co-transfected using Effectine transfection reagent (Qiagen) with a GFP-expressing plasmid (gift of Maria Blasi, Duke University) and a second plasmid encoding the full-length Towne strain gB (SinoBiological). Transfected cells were incubated for 2 days at 37°C and 5% CO_2, washed with DPBS (Gibco), then removed from the flask using enzyme free cell-dissociation buffer (ThermoFisher Scientific). Cells were washed in wash buffer (DPBS + 1% FBS), then 100,000 live cells were added to each well of a 96-well V-bottom plate (Corning). After centrifugation (1200 x g, 5 minutes), cells were re-suspended in 1:6250 diluted sera samples and incubated for 2 hours at 37°C and 5% CO_2. Next, cells were washed and stained with LIVE/DEAD Aqua Dead Cell Stain Kit (ThermoFisher Scientific) diluted 1:1000 for 20 minutes at RT. Afterwards, cells were washed, then re-suspended in PE-conjugated goat anti-human IgG Fc (eBioscience) diluted 1:200 in wash buffer then incubated for 25 minutes at 4°C. Following two additional wash steps, cells were re-suspended and fixed in DPBS + 1% formalin. Events were acquired on LSR Fortessa machine (BD biosciences) using the high-throughput sampler (HTS). The % PE+ cells was calculated from the live, GFP+ cell population

and reported for each sample. Background binding of each plasma sample was corrected for using cells transfected with the GFP-expressing plasmid alone.

Avidity ELISA. 384-well ELISA plates (Corning) were coated overnight at 4°C with 30 ng full-length gB per well, then blocked with assay diluent (1x PBS containing 4% whey, 15% normal goat serum, and 0.5% Tween-20). Three-fold dilutions of sera were then added to the plate, , then duplicate wells were treated for 5 min with either 7M urea or 1x PBS following sera incubation. Finally, bound IgG was detected with a horseradish peroxidase (HRP)-conjugated polyclonal goat anti-monkey IgG (Rockland), and developed using the SureBlue Reserve tetramethylbenzidine (TMB) peroxidase substrate (KPL). Sera dilutions that resulted in an OD value between 0.6 and 1.2 in the absence of urea treatment (dilution range = 1:30-1:1000) were used to determine the relative avidity index (RAI). Indexes were calculated as the OD ratio of urea:PBS treated wells.

Glycoprotein B peptide microarray. Binding to gB linear peptides was assessed as previously [15]. In brief, 15-mer peptides covering the entire gB open reading frame (Towne strain), and overlapping with neighboring peptides by 10 residues (total of 188 peptides) were synthesized and printed to a PepStar multiwell array (JPT Peptide) in triplicate. Microarray binding was performed manually using individual slides immobilized in the ArraySlide 24-4 chamber (JPT Peptide). First, arrays were blocked with blocking buffer (PBS containing 1% milk blotto, 5% NGS, and 0.05% Tween20), incubated first with sera diluted 1:250 in blocking buffer, and secondly with anti-human IgG conjugated to AF647 (Jackson ImmunoResearch) diluted in blocking buffer (0.75 µg/mL). Arrays were washed in wash buffer (1x TBS buffer + 0.1% Tween) between steps using an automated plate washer (BioTec ELX50). To measure fluorescence, arrays were scanned at a wavelength of 635 nm using an InnoScan 710 device (Innopsys) at a PMT setting of 580 and 100% laser power. Images were analyzed using Mapix software (Innopsys), and reviewed manually for accurate automated peptide identification. Binding intensity of sera to each peptide

was corrected with the surrounding background fluorescence. Median fluorescent intensity of each of the 3 replicates was reported.

Neutralization. The neutralization titers of patient sera were measured by both a high-throughput immunofluorescence assay as previously described [15]. Briefly, MRC-5 cells were seeded into 96-well flat-bottom plates and incubated for 2 days at 37°C and 5% CO2 to achieve 100% confluency. Once confluent, 3-fold dilutions (1:10–1:30,000) of heat-inactivated rabbit sera in infection media were incubated with an MOI=1.0 of Towne (ATCC) or AD169r (Merck Laboratories) virus stock in a total volume of 50 µL for 45 minutes at 37°C. For complement neutralization assays, plasma/virus was diluted in infection media containing rabbit complement (Cedarlane Laboratories) at a final dilution of 1:4. Immune complexes were added in duplicate to wells containing MRC-5 cells, then subsequently incubated for 18 hours at 37°C. Infected cells were then fixed for 10 minutes with 3.7% paraformaldehyde, permeabilized for 10 minutes with Triton × 100, and subsequently processed for immunofluorescence with mouse anti-HCMV IE-1 monoclonal antibody (MAB810, Millipore) followed by goat anti-mouse IgG-AlexaFluor488 (Millipore) and DAPI nuclear stain. Total cells and AF488+ infected cells per well were counted on a Cellomics Arrayscan (ThermoFisher Scientific). Neutralization titers (ID_{50}) were calculated according to the method of Reed and Muench using the plasma dilution that resulted in a 50% reduction in the percentage of infected cells compared to control wells infected with virus only.

Whole HCMV virion phagocytosis. The ability of vaccine-elicited antibodies to facilitate phagocytosis of whole HCMV virions was assessed as previously [15]. Briefly, 10^7 PFU of concentrated, sucrose gradient-purified HCMV TB40/E-mCherry virus was buffer exchanged with 1x PBS and sodium bicarbonate (0.1M final concentration), then AF647 NHS ester (Invitrogen) added for direct viral conjugation at room temperature for 1 hour with constant agitation. The reaction was quenched with 1 M Tris-HCl, pH 8.0, then the labelled virus was diluted 25x in wash

buffer (PBS + 0.1% FBS). Sera samples were diluted 1:10 in wash buffer, then 10 µL of diluted sera combined with 10 µL of diluted, fluorophore-conjugated virus in a round-bottom, 96-well plate (Corning) and allowed to incubate at 37°C for 2 hours. Following this incubation step, 25,000 THP-1 cells were added to each well, suspended in 200 µL primary growth media. Plates were centrifuged at 1200 xg and 4°C for 1 hour in a spinoculation step, then incubated at 37°C for an additional hour. Cells were re-suspended and transferred to a 96-well V-bottom plate, then washed twice prior to fixing in 100µL DPBS + 1% formalin. Events were acquired on LSR Fortessa machine (BD biosciences) using the HTS. The % AF647+ cells was calculated from the full THP-1 cell population and reported for each sample. A cutoff for sample positivity was defined as the mean value of pre-vaccination sera (n=18) + 2 standard deviations.

Natural killer (NK) cell CD107a degranulation assay. Cell-surface expression of CD107a was used as a marker for NK cell degranulation, which we have previously shown to have good agreement with antibody-dependent cellular cytotoxicity activity for rabbit sera [17]. MRC-5 cells were infected with BadrUL131-Y4 with a MOI of 1.0 for 48 hours at 37°C, at $4x10^4$ cells/well in 96-well flat-bottom tissue culture plates. Following incubation, supernatant was removed and the infected cell monolayers were washed once with RMPI 1640 containing 10% FBS, HEPES, Pen-Strep-L-Glut, Gentamicin (R10 media) before addition of NK cells. Primary human NK cells were isolated from peripheral blood mononuclear cells (PBMC) after overnight rest in R10 media with 10ng/mL IL-15 (Miltenyi Biotech) by depletion of magnetically labeled cells (Human NK cell isolation kit, Miltenyi Biotech). $5x10^4$ live NK cells were added to each well containing HCMV-infected MRC-5 cell monolayers. Plasma samples were diluted in R10 and added to the cells at a final dilution of 1:50 in duplicate. Brefeldin A (GolgiPlug, 1 µl/ml, BD Biosciences), monensin (GolgiStop, 4µl/6mL, BD Biosciences), and CD107a-FITC (BD Biosciences, clone H4A3) were added to each well and the plates were incubated for 6 hours at 37oC in a humidified 5% CO_2 incubator. NK cells were then gently resuspended, taking care not to disturb the MRC-5 cell

534 monolayer, and the NK containing supernatant was collected and transferred to 96-well V-bottom
535 plates. The recovered NK cells were washed with PBS, and stained with LIVE/DEAD Aqua Dead
536 Cell Stain at a 1:1000 dilution for 20 minutes at room temperature. The cells were then washed
537 with 1%FBS PBS and stained for 20 minutes at room temperature with the following panel of
538 fluorescently conjugated antibodies diluted in 1%FBS PBS: CD56-PECy7 (BD Biosciences, clone
539 NCAM16.2), CD16-PacBlue (BD Biosciences, clone 3G8), and CD69-BV785 (BioLegend, Clone
540 FN50). The cells were then washed twice and re-suspended in 1% paraformaldehyde fixative for
541 flow cytometric analysis. Data analysis was performed using FlowJo software (v9.9.6). Data is
542 reported as the % of CD107a positive live NK cells (singlets, lymphocytes, aqua blue^{-}, CD56^{+}
543 and/or CD16^{+}, CD107a^{+}). CD69 was not used in the final analysis due to the low frequency of
544 CD107a+ responses. Parallel assays were performed with uninfected MRC-5 cells as a control
545 for identification of non-CMV specific responses, and final data are presented after subtraction of
546 background activity observed against uninfected cells.
547
548 *Soluble protein bead coupling and antibody depletion.* Cyanogen bromide-activated (CNBr-
549 activated) sepharose beads (GE Healthcare) were rehydrated with 1 mM HCl then suspended in
550 coupling buffer (0.1 M $NaHCO_3$ + 0.5 M NaCl, pH 8.3). Every 100 µL of bead slurry was combined
551 with 200 µg of soluble gB ectodomain (post-fusion conformation, courtesy of Jason McLellan,
552 University of Texas, Austin). Coupling proceeded for 12 hours at 4°C on an inversion rotator.
553 Excess soluble protein was washed off with 5 column volumes of coupling buffer. Unbound CNBr
554 active groups were blocked with quenching buffer (0.1 M Tris HCl pH 8.0) for 2 hours at room
555 temperature. Protein conjugated beads were washed with 3 cycles of alternating pH 0.1 M acetic
556 acid, pH 4.0 and 0.1 M Tris HCl pH 8. For depletion of gB post fusion specific antibodies, 100 µg
557 of protein-coupled bead slurry was loaded into a spin microelution column (Pierce, TFS). 400 µL
558 of filtered (SpinX) 1:50 diluted plasma from vaccinated rabbits was then added to each column.

559 Plasma was centrifuged through the column 10 times with bound IgG elution (0.2 M glycine elution
560 buffer, pH 2.5) and bead recalibration (3 cycles of alternating pH washes) after spins 5 and 10.
561 Adequate specific depletion was confirmed by ELISA against the depleted protein. Mock depleted
562 samples underwent an identical depletion procedure in the presence of HIV-1 gp120 conjugated
563 CNBr beads.
564
565 *Splenic T cell intracellular cytokine staining.* Primary spleen cells were thawed in RPMI + 10%
566 FBS with benzonase (50 U/mL) then measured for count and viability on Muse Cell Counter
567 (Luminex). Cells were coincubated in duplicate with Con A (5ug/mL), HCMV UL155 (250ng/mL.
568 JPT), or media for 20-24 hours at 37 degrees C. Samples were stained for rabbit pan-T cell marker
569 KEN-5 (SCBT) and live/dead (Invitrogen), then fixed and permeabilized using BD
570 Cytofix/Cytoperm according to the manufacturer's instructions. Cells were stained for rabbit IFN-
571 γ (mAb Tech). Flow cytometry was performed on a BD LSR II, and data was analyzed in Flow Jo
572 v10. Gating strategy shown in **Figure S4**.
573
574 *Statistical analysis.* Nonparametric tests were utilized because of the small group sizes (n=6 per
575 group). Furthermore, the 20 week timepoint was employed for all statistical comparisons between
576 vaccination groups. Magnitude of immune responses between the 3 vaccine groups were
577 compared first by Kruskal-Wallis test. If $p<0.05$, *post hoc* Mann-Whitney U test was conducted for
578 gB ecto and gB mRNA compared with gB FL. All statistical tests were carried out using the R
579 statistical interface (version 3.3.1, www.r-project.org) and were two-tailed.
580
581 *Ethics statement*. Animals were maintained in accordance with the American Association for
582 Accreditation of Laboratory Animal Care standards and *The Guide for the Care and Use of*
583 *Laboratory Animals* [58]. Efforts were made to minimize stress and provide enrichment
584 opportunities when possible (social housing when possible, objects to manipulate in cage, varied

585 food supplements, interaction with caregivers and research staff). All protocols were reviewed
586 and approved by the Duke University Animal Care and Use Committee (IACUC) prior to the
587 initiation of the study (protocol #A314-15-12).

588 **Author contributions:**

589 C.S.N. and S.R.P. designed research; C.S.N., J.A.J., N.P., H.R., M.G., and W.E. performed

590 research; C.S.N. analyzed data; D.W., J.M., and J.P. contributed reagents and expertise; C.S.N.

591 and S.R.P. wrote the paper.

Acknowledgements:

The authors would like to thank Diego Zapata and the Duke Division of Laboratory and Animal Resources for assistance with rabbit handling. Furthermore, we acknowledge Sanofi-Pasteur, Merck, and Trellis Biosciences for the generous gift of research materials. This work was supported by: NIH/NIAID R21 to S.R.P (R21AI136556) and NIH/NICHD F30 grant to C.S.N (F30HD089577). The funders had no role in study design, data collection and interpretation, decision to publish, or the preparation of this manuscript. The content is solely the responsibility of the authors and does not necessarily represent the official views of the National Institutes of Health.

References:

1. Swanson EC, Gillis P, Hernandez-Alvarado N, Fernandez-Alarcon C, Schmit M, Zabeli JC, et al. Comparison of monovalent glycoprotein B with bivalent gB/pp65 (GP83) vaccine for congenital cytomegalovirus infection in a guinea pig model: Inclusion of GP83 reduces gB antibody response but both vaccine approaches provide equivalent protection against pup mortality. Vaccine. 2015;33(32):4013-8. doi: 10.1016/j.vaccine.2015.06.019. PubMed PMID: 26079615; PubMed Central PMCID: PMCPMC4772145.
2. Manicklal S, Emery VC, Lazzarotto T, Boppana SB, Gupta RK. The "Silent" Global Burden of Congenital Cytomegalovirus. Clinical Microbiology Reviews. 2013;26(1):86-102. doi: 10.1128/Cmr.00062-12. PubMed PMID: WOS:000313344900005.
3. Kenneson A, Cannon MJ. Review and meta-analysis of the epidemiology of congenital cytomegalovirus (CMV) infection. Rev Med Virol. 2007;17(4):253-76. doi: 10.1002/rmv.535. PubMed PMID: 17579921.
4. Ross SA, Boppana SB. Congenital cytomegalovirus infection: outcome and diagnosis. Semin Pediatr Infect Dis. 2005;16(1):44-9. doi: 10.1053/j.spid.2004.09.011. PubMed PMID: 15685149.
5. Legendre C, Pascual M. Improving outcomes for solid-organ transplant recipients at risk from cytomegalovirus infection: late-onset disease and indirect consequences. Clin Infect Dis. 2008;46(5):732-40. Epub 2008/01/29. doi: 10.1086/527397. PubMed PMID: 18220478.
6. Ljungman P, Griffiths P, Paya C. Definitions of cytomegalovirus infection and disease in transplant recipients. Clin Infect Dis. 2002;34(8):1094-7. Epub 2002/03/27. doi: 10.1086/339329. PubMed PMID: 11914998.
7. Bialas KM, Permar SR. The March towards a Vaccine for Congenital CMV: Rationale and Models. PLoS pathogens. 2016;12(2):e1005355. doi: 10.1371/journal.ppat.1005355. PubMed PMID: 26866914; PubMed Central PMCID: PMCPMC4750955.
8. Griffiths PD. Burden of disease associated with human cytomegalovirus and prospects for elimination by universal immunisation. The Lancet Infectious diseases. 2012;12(10):790-8. Epub 2012/09/29. doi: 10.1016/S1473-3099(12)70197-4. PubMed PMID: 23017365.
9. Schleiss MR. Recombinant cytomegalovirus glycoprotein B vaccine: Rethinking the immunological basis of protection. Proceedings of the National Academy of Sciences of the United States of America. 2018;115(24):6110-2. Epub 2018/06/08. doi: 10.1073/pnas.1806420115. PubMed PMID: 29875141; PubMed Central PMCID: PMCPMC6004476.
10. Vanarsdall AL, Johnson DC. Human cytomegalovirus entry into cells. Curr Opin Virol. 2012;2(1):37-42. doi: 10.1016/j.coviro.2012.01.001. PubMed PMID: 22440964; PubMed Central PMCID: PMCPMC3880194.
11. Zydek M, Petitt M, Fang-Hoover J, Adler B, Kauvar LM, Pereira L, et al. HCMV infection of human trophoblast progenitor cells of the placenta is neutralized by a human monoclonal antibody to glycoprotein B and not by antibodies to the pentamer complex. Viruses. 2014;6(3):1346-64. doi: 10.3390/v6031346. PubMed PMID: 24651029; PubMed Central PMCID: PMCPMC3970154.
12. Pass RF, Zhang C, Evans A, Simpson T, Andrews W, Huang ML, et al. Vaccine prevention of maternal cytomegalovirus infection. The New England journal of medicine. 2009;360(12):1191-9. doi: 10.1056/NEJMoa0804749. PubMed PMID: 19297572; PubMed Central PMCID: PMCPMC2753425.
13. Bernstein DI, Munoz FM, Callahan ST, Rupp R, Wootton SH, Edwards KM, et al. Safety and efficacy of a cytomegalovirus glycoprotein B (gB) vaccine in adolescent girls: A randomized clinical trial. Vaccine. 2016;34(3):313-9. doi: 10.1016/j.vaccine.2015.11.056. PubMed PMID: 26657184; PubMed Central PMCID: PMCPMC4701617.

14. Griffiths PD, Stanton A, McCarrell E, Smith C, Osman M, Harber M, et al. Cytomegalovirus glycoprotein-B vaccine with MF59 adjuvant in transplant recipients: a phase 2 randomised placebo-controlled trial. Lancet. 2011;377(9773):1256-63. Epub 2011/04/13. doi: 10.1016/S0140-6736(11)60136-0. PubMed PMID: 21481708; PubMed Central PMCID: PMCPMC3075549.
15. Nelson CS, Huffman T, Jenks JA, Cisneros de la Rosa E, Xie G, Vandergrift N, et al. HCMV glycoprotein B subunit vaccine efficacy mediated by nonneutralizing antibody effector functions. Proceedings of the National Academy of Sciences of the United States of America. 2018. Epub 2018/05/02. doi: 10.1073/pnas.1800177115. PubMed PMID: 29712861.
16. Baraniak I, Kropff B, Ambrose L, McIntosh M, McLean GR, Pichon S, et al. Protection from cytomegalovirus viremia following glycoprotein B vaccination is not dependent on neutralizing antibodies. Proceedings of the National Academy of Sciences of the United States of America. 2018;115(24):6273-8. Epub 2018/04/25. doi: 10.1073/pnas.1800224115. PubMed PMID: 29686064; PubMed Central PMCID: PMCPMC6004462.
17. Pollara J, Jones DI, Huffman T, Edwards RW, Dennis M, Li SH, et al. Bridging Vaccine-Induced HIV-1 Neutralizing and Effector Antibody Responses in Rabbit and Rhesus Macaque Animal Models. Journal of virology. 2019;93(10). Epub 2019/03/08. doi: 10.1128/JVI.02119-18. PubMed PMID: 30842326.
18. Nelson CS HT, Cisneros de la Rosa E, Xi G, Vandergrift N, Pass RF, Pollara J, Permar SR. HCMV glycoprotein B subunit vaccine efficacy was mediated by non-neutralizing antibody effector functions. bioRxiv: preprint server for biololgy. 2018. Epub 12 January 2018. doi: https://doi.org/10.1101/246884.
19. Baraniak I, Kropff B, McLean GR, Pichon S, Piras-Douce F, Milne RSB, et al. Epitope-Specific Humoral Responses to Human Cytomegalovirus Glycoprotein-B Vaccine With MF59: Anti-AD2 Levels Correlate With Protection From Viremia. The Journal of infectious diseases. 2018;217(12):1907-17. Epub 2018/03/13. doi: 10.1093/infdis/jiy102. PubMed PMID: 29528415; PubMed Central PMCID: PMCPMC5972559.
20. Bialas KM, Westreich D, Cisneros de la Rosa E, Nelson CS, Kauvar LM, Fu TM, et al. Maternal Antibody Responses and Nonprimary Congenital Cytomegalovirus Infection of HIV-1-Exposed Infants. The Journal of infectious diseases. 2016;214(12):1916-23. Epub 2016/12/08. doi: 10.1093/infdis/jiw487. PubMed PMID: 27923951; PubMed Central PMCID: PMCPMC5142097.
21. Pardi N, Hogan MJ, Naradikian MS, Parkhouse K, Cain DW, Jones L, et al. Nucleoside-modified mRNA vaccines induce potent T follicular helper and germinal center B cell responses. The Journal of experimental medicine. 2018;215(6):1571-88. Epub 2018/05/10. doi: 10.1084/jem.20171450. PubMed PMID: 29739835; PubMed Central PMCID: PMCPMC5987916.
22. Macagno A, Bernasconi NL, Vanzetta F, Dander E, Sarasini A, Revello MG, et al. Isolation of human monoclonal antibodies that potently neutralize human cytomegalovirus infection by targeting different epitopes on the gH/gL/UL128-131A complex. Journal of virology. 2010;84(2):1005-13. doi: 10.1128/JVI.01809-09. PubMed PMID: 19889756; PubMed Central PMCID: PMCPMC2798344.
23. Fouts AE, Chan P, Stephan JP, Vandlen R, Feierbach B. Antibodies against the gH/gL/UL128/UL130/UL131 complex comprise the majority of the anti-cytomegalovirus (anti-CMV) neutralizing antibody response in CMV hyperimmune globulin. Journal of virology. 2012;86(13):7444-7. doi: 10.1128/JVI.00467-12. PubMed PMID: 22532696; PubMed Central PMCID: PMCPMC3416310.
24. Nelson CS, Herold BC, Permar SR. A new era in cytomegalovirus vaccinology: considerations for rational design of next-generation vaccines to prevent congenital cytomegalovirus infection. NPJ Vaccines. 2018;3:38. Epub 2018/10/03. doi: 10.1038/s41541-018-0074-4. PubMed PMID: 30275984; PubMed Central PMCID: PMCPMC6148244 preclinical

HCMV vaccine programs. B.C.H. is an inventor on a pending patent application for a delta gD-2 vaccine. The other authors have no conflicts of interest to declare.

25. Nelson CS, Huffman T, Jenks JA, Cisneros de la Rosa E, Xie G, Vandergrift N, et al. HCMV glycoprotein B subunit vaccine efficacy mediated by nonneutralizing antibody effector functions. Proceedings of the National Academy of Sciences of the United States of America. 2018;115(24):6267-72. Epub 2018/05/02. doi: 10.1073/pnas.1800177115. PubMed PMID: 29712861; PubMed Central PMCID: PMCPMC6004431.

26. Bialas KM, Tanaka T, Tran D, Varner V, Cisneros De La Rosa E, Chiuppesi F, et al. Maternal CD4+ T cells protect against severe congenital cytomegalovirus disease in a novel nonhuman primate model of placental cytomegalovirus transmission. Proceedings of the National Academy of Sciences of the United States of America. 2015;112(44):13645-50. Epub 2015/10/21. doi: 10.1073/pnas.1511526112. PubMed PMID: 26483473; PubMed Central PMCID: PMCPMC4640765.

27. Itell HL, Kaur A, Deere JD, Barry PA, Permar SR. Rhesus monkeys for a nonhuman primate model of cytomegalovirus infections. Curr Opin Virol. 2017;25:126-33. Epub 2017/09/10. doi: 10.1016/j.coviro.2017.08.005. PubMed PMID: 28888133; PubMed Central PMCID: PMCPMC5659282.

28. Boppana SB, Britt WJ. Antiviral Antibody Responses and Intrauterine Transmission after Primary Maternal Cytomegalovirus Infection. Journal of Infectious Diseases. 1995;171(5):1115-21. doi: 10.1093/infdis/171.5.1115.

29. Nelson CS, Cruz DV, Tran D, Bialas KM, Stamper L, Wu H, et al. Preexisting antibodies can protect against congenital cytomegalovirus infection in monkeys. JCI Insight. 2017;2(13). doi: 10.1172/jci.insight.94002. PubMed PMID: 28679960; PubMed Central PMCID: PMCPMC5499366.

30. Bootz A, Karbach A, Spindler J, Kropff B, Reuter N, Sticht H, et al. Protective capacity of neutralizing and non-neutralizing antibodies against glycoprotein B of cytomegalovirus. PLoS pathogens. 2017;13(8):e1006601. Epub 2017/08/31. doi: 10.1371/journal.ppat.1006601. PubMed PMID: 28854233; PubMed Central PMCID: PMCPMC5595347.

31. Forthal DN, Phan T, Landucci G. Antibody inhibition of cytomegalovirus: the role of natural killer and macrophage effector cells. Transpl Infect Dis. 2001;3 Suppl 2:31-4. PubMed PMID: 11926747.

32. Chen SF, Holmes TH, Slifer T, Ramachandran V, Mackey S, Hebson C, et al. Longitudinal Kinetics of Cytomegalovirus-Specific T-Cell Immunity and Viral Replication in Infants With Congenital Cytomegalovirus Infection. J Pediatric Infect Dis Soc. 2016;5(1):14-20. Epub 2016/02/26. doi: 10.1093/jpids/piu089. PubMed PMID: 26908487; PubMed Central PMCID: PMCPMC4765489.

33. Hansen SG, Powers CJ, Richards R, Ventura AB, Ford JC, Siess D, et al. Evasion of CD8+ T cells is critical for superinfection by cytomegalovirus. Science. 2010;328(5974):102-6. Epub 2010/04/03. doi: 10.1126/science.1185350. PubMed PMID: 20360110; PubMed Central PMCID: PMCPMC2883175.

34. Gamadia LE, Rentenaar RJ, van Lier RA, ten Berge IJ. Properties of CD4(+) T cells in human cytomegalovirus infection. Hum Immunol. 2004;65(5):486-92. Epub 2004/06/03. doi: 10.1016/j.humimm.2004.02.020. PubMed PMID: 15172448.

35. Gerna G, Lilleri D, Fornara C, Bruno F, Gabanti E, Cane I, et al. Differential kinetics of human cytomegalovirus load and antibody responses in primary infection of the immunocompetent and immunocompromised host. J Gen Virol. 2015;96(Pt 2):360-9. Epub 2014/10/16. doi: 10.1099/vir.0.070441-0. PubMed PMID: 25316796.

36. Widmann T, Sester U, Gartner BC, Schubert J, Pfreundschuh M, Kohler H, et al. Levels of CMV specific CD4 T cells are dynamic and correlate with CMV viremia after allogeneic stem cell transplantation. PloS one. 2008;3(11):e3634. Epub 2008/11/05. doi:

752 10.1371/journal.pone.0003634. PubMed PMID: 18982061; PubMed Central PMCID:
753 PMCPMC2572846.
754 37. Lilleri D, Fornara C, Furione M, Zavattoni M, Revello MG, Gerna G. Development of
755 human cytomegalovirus-specific T cell immunity during primary infection of pregnant women
756 and its correlation with virus transmission to the fetus. The Journal of infectious diseases.
757 2007;195(7):1062-70. Epub 2007/03/03. doi: 10.1086/512245. PubMed PMID: 17330798.
758 38. Revello MG, Lilleri D, Zavattoni M, Furione M, Genini E, Comolli G, et al.
759 Lymphoproliferative response in primary human cytomegalovirus (HCMV) infection is delayed in
760 HCMV transmitter mothers. The Journal of infectious diseases. 2006;193(2):269-76. Epub
761 2005/12/20. doi: 10.1086/498872. PubMed PMID: 16362891.
762 39. Saldan A, Forner G, Mengoli C, Gussetti N, Palu G, Abate D. Strong Cell-Mediated
763 Immune Response to Human Cytomegalovirus Is Associated With Increased Risk of Fetal
764 Infection in Primarily Infected Pregnant Women. Clin Infect Dis. 2015;61(8):1228-34. Epub
765 2015/07/16. doi: 10.1093/cid/civ561. PubMed PMID: 26175520.
766 40. Lilleri D, Zelini P, Fornara C, Zavaglio F, Rampino T, Perez L, et al. Human
767 cytomegalovirus (HCMV)-specific T cell but not neutralizing or IgG binding antibody responses
768 to glycoprotein complexes gB, gHgLgO, and pUL128L correlate with protection against high
769 HCMV viral load reactivation in solid-organ transplant recipients. J Med Virol. 2018;90(10):1620-
770 8. Epub 2018/05/26. doi: 10.1002/jmv.25225. PubMed PMID: 29797330.
771 41. Aubert G, Hassan-Walker AF, Madrigal JA, Emery VC, Morte C, Grace S, et al.
772 Cytomegalovirus-specific cellular immune responses and viremia in recipients of allogeneic
773 stem cell transplants. The Journal of infectious diseases. 2001;184(8):955-63. Epub
774 2001/09/28. doi: 10.1086/323354. PubMed PMID: 11574909.
775 42. Sacre K, Carcelain G, Cassoux N, Fillet AM, Costagliola D, Vittecoq D, et al. Repertoire,
776 diversity, and differentiation of specific CD8 T cells are associated with immune protection
777 against human cytomegalovirus disease. The Journal of experimental medicine.
778 2005;201(12):1999-2010. Epub 2005/06/22. doi: 10.1084/jem.20042408. PubMed PMID:
779 15967826; PubMed Central PMCID: PMCPMC2212029.
780 43. Gabanti E, Bruno F, Lilleri D, Fornara C, Zelini P, Cane I, et al. Human cytomegalovirus
781 (HCMV)-specific CD4+ and CD8+ T cells are both required for prevention of HCMV disease in
782 seropositive solid-organ transplant recipients. PloS one. 2014;9(8):e106044. Epub 2014/08/29.
783 doi: 10.1371/journal.pone.0106044. PubMed PMID: 25166270; PubMed Central PMCID:
784 PMCPMC4148399.
785 44. Snyder LD, Chan C, Kwon D, Yi JS, Martissa JA, Copeland CA, et al. Polyfunctional T-
786 Cell Signatures to Predict Protection from Cytomegalovirus after Lung Transplantation. Am J
787 Respir Crit Care Med. 2016;193(1):78-85. Epub 2015/09/16. doi: 10.1164/rccm.201504-
788 0733OC. PubMed PMID: 26372850; PubMed Central PMCID: PMCPMC4731614.
789 45. Pardi N, Hogan MJ, Pelc RS, Muramatsu H, Andersen H, DeMaso CR, et al. Zika virus
790 protection by a single low-dose nucleoside-modified mRNA vaccination. Nature.
791 2017;543(7644):248-51. doi: 10.1038/nature21428. PubMed PMID: 28151488; PubMed Central
792 PMCID: PMCPMC5344708.
793 46. Pardi N, Hogan MJ, Porter FW, Weissman D. mRNA vaccines - a new era in
794 vaccinology. Nat Rev Drug Discov. 2018;17(4):261-79. Epub 2018/01/13. doi:
795 10.1038/nrd.2017.243. PubMed PMID: 29326426; PubMed Central PMCID: PMCPMC5906799.
796 47. Pardi N, Parkhouse K, Kirkpatrick E, McMahon M, Zost SJ, Mui BL, et al. Nucleoside-
797 modified mRNA immunization elicits influenza virus hemagglutinin stalk-specific antibodies.
798 Nature communications. 2018;9(1):3361. Epub 2018/08/24. doi: 10.1038/s41467-018-05482-0.
799 PubMed PMID: 30135514; PubMed Central PMCID: PMCPMC6105651.
800 48. John S, Yuzhakov O, Woods A, Deterling J, Hassett K, Shaw CA, et al. Multi-antigenic
801 human cytomegalovirus mRNA vaccines that elicit potent humoral and cell-mediated immunity.

802 Vaccine. 2018;36(12):1689-99. Epub 2018/02/20. doi: 10.1016/j.vaccine.2018.01.029. PubMed
803 PMID: 29456015.
804 49. Pardi N, Tuyishime S, Muramatsu H, Kariko K, Mui BL, Tam YK, et al. Expression
805 kinetics of nucleoside-modified mRNA delivered in lipid nanoparticles to mice by various routes.
806 J Control Release. 2015;217:345-51. Epub 2015/08/13. doi: 10.1016/j.jconrel.2015.08.007.
807 PubMed PMID: 26264835; PubMed Central PMCID: PMCPMC4624045.
808 50. Lambert PH, Laurent PE. Intradermal vaccine delivery: will new delivery systems
809 transform vaccine administration? Vaccine. 2008;26(26):3197-208. Epub 2008/05/20. doi:
810 10.1016/j.vaccine.2008.03.095. PubMed PMID: 18486285.
811 51. Pardi N, Muramatsu H, Weissman D, Kariko K. In vitro transcription of long RNA
812 containing modified nucleosides. Methods in molecular biology. 2013;969:29-42. Epub
813 2013/01/09. doi: 10.1007/978-1-62703-260-5_2. PubMed PMID: 23296925.
814 52. Thess A, Grund S, Mui BL, Hope MJ, Baumhof P, Fotin-Mleczek M, et al. Sequence-
815 engineered mRNA Without Chemical Nucleoside Modifications Enables an Effective Protein
816 Therapy in Large Animals. Mol Ther. 2015;23(9):1456-64. Epub 2015/06/09. doi:
817 10.1038/mt.2015.103. PubMed PMID: 26050989; PubMed Central PMCID: PMCPMC4817881.
818 53. Weissman D, Pardi N, Muramatsu H, Kariko K. HPLC purification of in vitro transcribed
819 long RNA. Methods in molecular biology. 2013;969:43-54. Epub 2013/01/09. doi: 10.1007/978-
820 1-62703-260-5_3. PubMed PMID: 23296926.
821 54. Maier MA, Jayaraman M, Matsuda S, Liu J, Barros S, Querbes W, et al. Biodegradable
822 lipids enabling rapidly eliminated lipid nanoparticles for systemic delivery of RNAi therapeutics.
823 Mol Ther. 2013;21(8):1570-8. Epub 2013/06/27. doi: 10.1038/mt.2013.124. PubMed PMID:
824 23799535; PubMed Central PMCID: PMCPMC3734658.
825 55. Jayaraman M, Ansell SM, Mui BL, Tam YK, Chen J, Du X, et al. Maximizing the potency
826 of siRNA lipid nanoparticles for hepatic gene silencing in vivo. Angew Chem Int Ed Engl.
827 2012;51(34):8529-33. Epub 2012/07/12. doi: 10.1002/anie.201203263. PubMed PMID:
828 22782619; PubMed Central PMCID: PMCPMC3470698.
829 56. Wang D, Li F, Freed DC, Finnefrock AC, Tang A, Grimes SN, et al. Quantitative analysis
830 of neutralizing antibody response to human cytomegalovirus in natural infection. Vaccine.
831 2011;29(48):9075-80. doi: 10.1016/j.vaccine.2011.09.056. PubMed PMID: 21945962.
832 57. Wang D, Yu QC, Schroer J, Murphy E, Shenk T. Human cytomegalovirus uses two
833 distinct pathways to enter retinal pigmented epithelial cells. Proceedings of the National
834 Academy of Sciences of the United States of America. 2007;104(50):20037-42. Epub
835 2007/12/14. doi: 10.1073/pnas.0709704104. PubMed PMID: 18077432; PubMed Central
836 PMCID: PMCPMC2148418.
837 58. In: th, editor. Guide for the Care and Use of Laboratory Animals. The National
838 Academies Collection: Reports funded by National Institutes of Health. Washington (DC)2011.

839

840 **Figures and Figure Legends:**

841

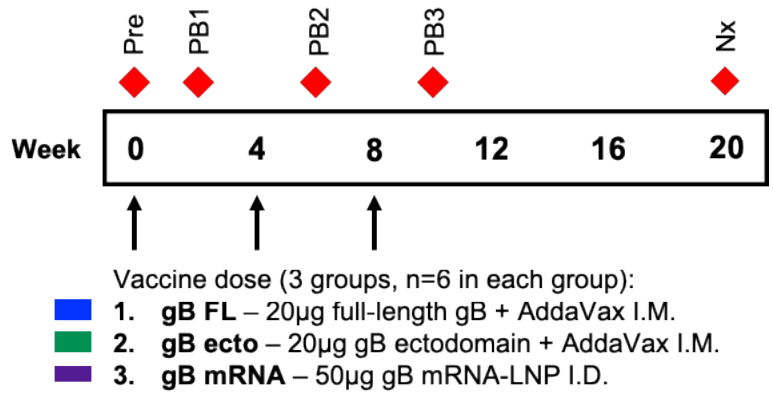

842

843 **Figure 1. Vaccination and sampling timeline.** At 0, 4, and 8 weeks, juvenile New Zealand White
844 rabbits were administered 50µg doses of either full-length gB protein + AddaVax intramuscularly
845 (blue), gB ectodomain protein + AddaVax intramuscularly (green), or lipid nanoparticle-packaged
846 gB mRNA intradermally (purple). Blood was sampled at the following timepoints indicated by red
847 diamonds: preimmune (0 weeks; 'Pre'), post boost 1 (2 weeks, 'PB1'), post boost 2 (6 weeks,
848 'PB2'), post boost 3 (10 weeks, 'PB3'), and necropsy (20 weeks, 'Nx').

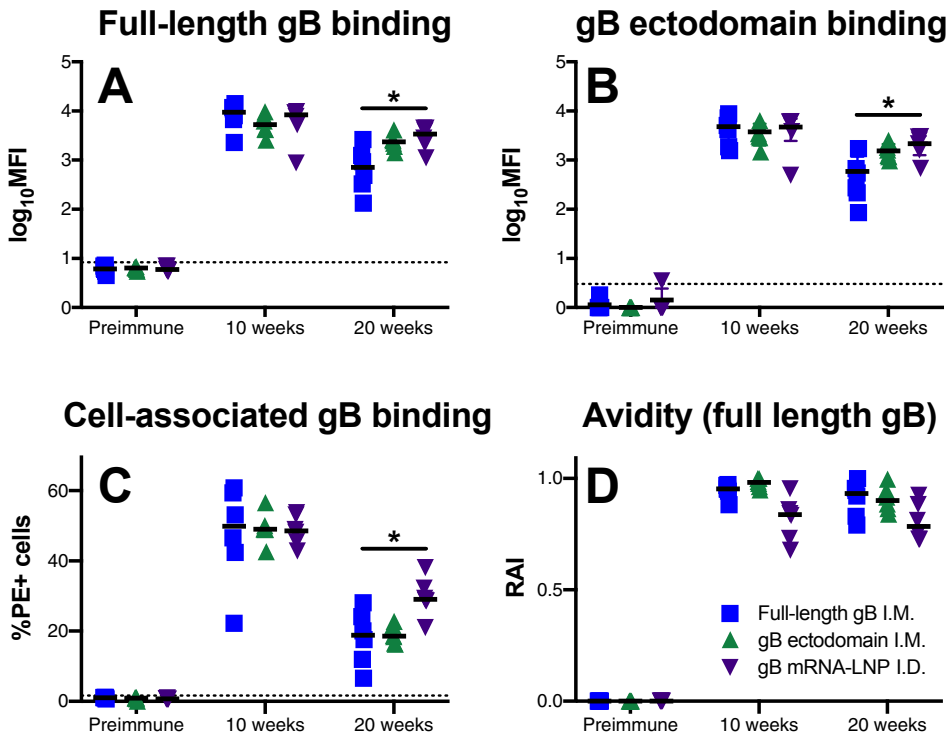

Figure 2. gB mRNA-LNP vaccination elicits more durable binding antibody responses against soluble and cell-associated gB. IgG binding to full-length gB (A) and gB ectodomain (B) proteins were assessed by BAMA. IgG binding to gB-transfected cells (C) was measured by flow cytometry. gB binding avidity was assessed against full-length gB using urea-wash ELISA. All proteins were strain-matched (Towne). IgG responses for full-length gB vaccinees are shown in blue, gB ectodomain in green, and gB mRNA-LNP in purple. Binding responses were assessed for preimmune, 10 week (post boost 3, peak immunogenicity), and 20 week (necropsy) timepoints. Data points represent individual animals, with the line designating the median. Dotted black line indicates the mean preimmune response + 2 standard deviations. *p<0.05, Kruskal-Wallis + *post hoc* Mann-Whitney U test.

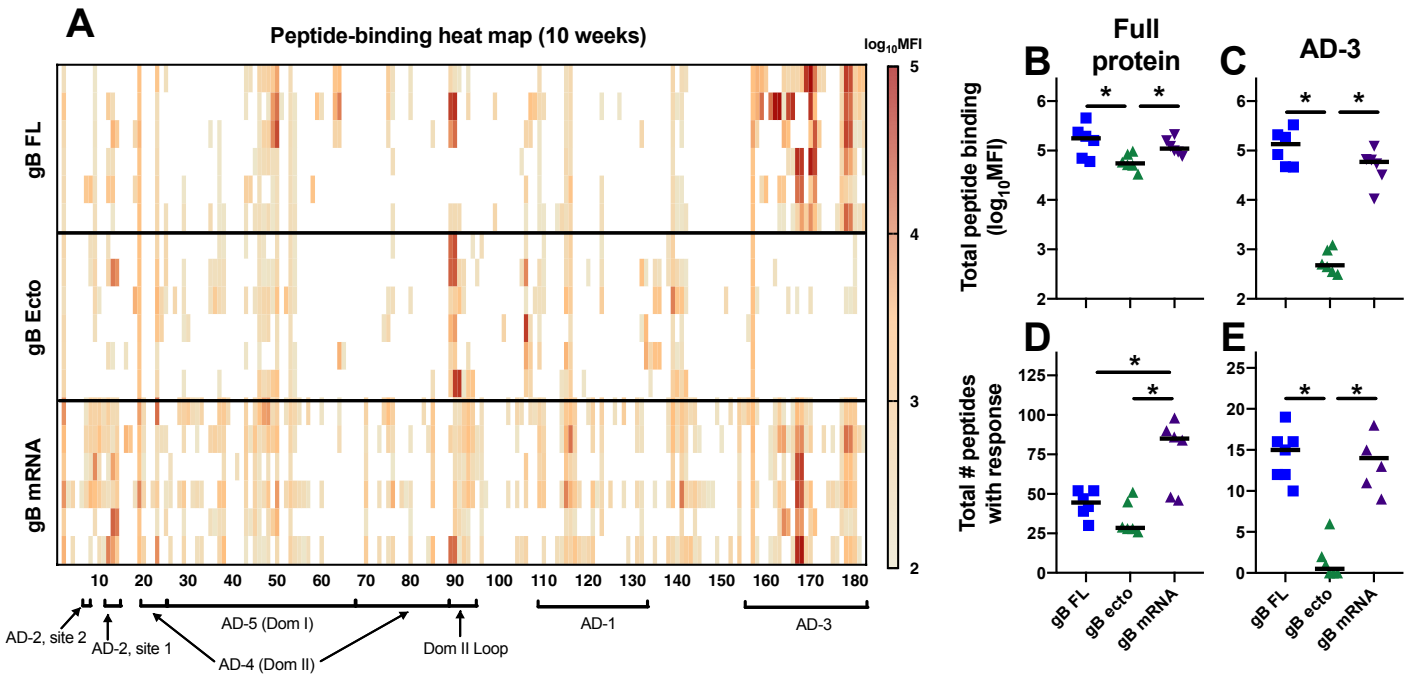

Figure 3. gB mRNA-LNP vaccination reduced AD-3 immunodominance, yet enhances breadth of linear peptide binding IgG response. (A) The binding magnitude of rabbit antibodies at week 10 (post boost 3, peak immunogenicity) were assessed against a 15-mer peptide library spanning the entire Towne gB ORF (180 unique peptides). Each row indicates a single rabbit. Peptides corresponding to distinct gB antigenic domains are indicated along the x-axis. (B,C) The sum of total peptide-binding MFI to both the full gB protein (B) and those peptide corresponding to the AD-3 epitope (C). (D,E) Number of unique peptides with a binding response >100 MFI for the full gB protein (C) and AD-3 epitope (E). Responses for full-length gB vaccinees are shown in blue, gB ectodomain in green, and gB mRNA-LNP in purple. Data points represent individual animals, with the line designating the median. *p<0.05, Kruskal-Wallis + *post hoc* Mann-Whitney U test.

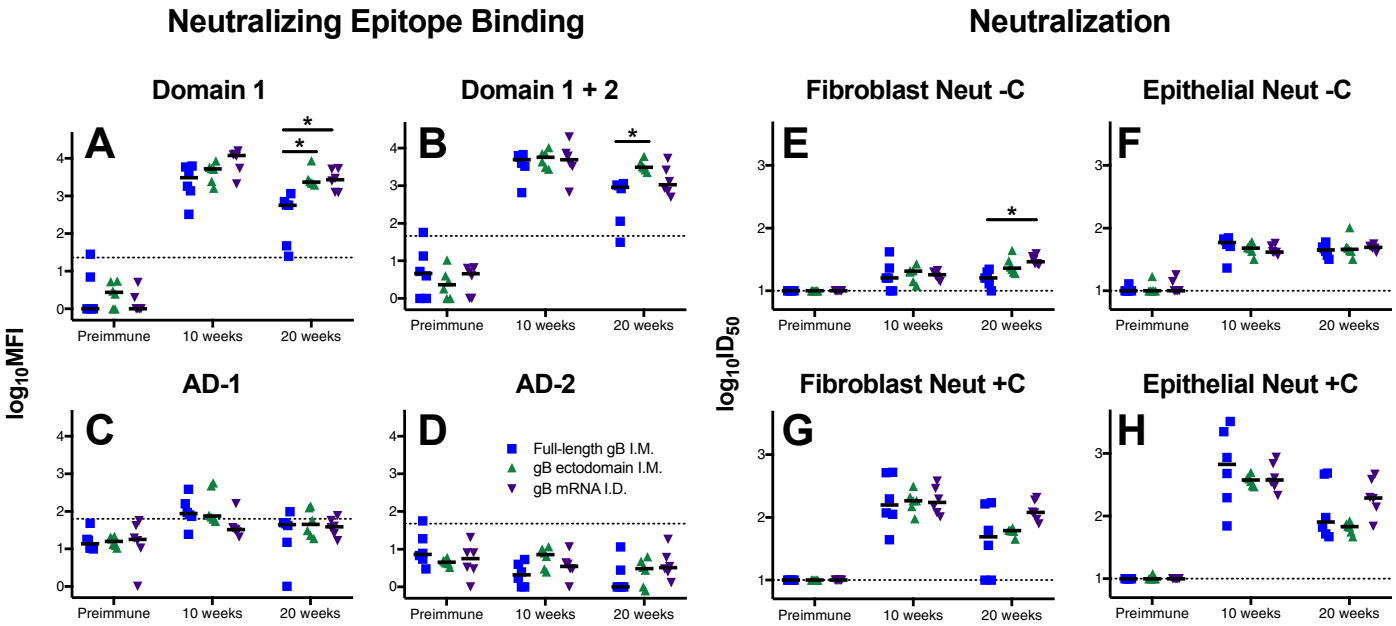

872

873 **Figure 4. Enhanced durability of HCMV-neutralizing antibodies following gB mRNA-LNP**
874 **vaccination.** Vaccine-elicited binding to glycoprotein B neutralizing epitopes domain 1 (A),
875 domain 1+2 (B), AD-1 (C), and AD-2 site 1 (D) was assessed by BAMA. Neutralization of
876 heterologous virus AD169r in the absence (-C; E-F) and presence (+C; G-H) of purified rabbit
877 complement on MRC-5 fibroblast cells (E,G) and ARPE epithelial cells (F,H). Full-length gB
878 vaccinees are shown in blue, gB ectodomain in green, and gB mRNA-LNP in purple. Antibody
879 responses were assessed for preimmune, 10 week (post boost 3, peak immunogenicity), and 20
880 week (necropsy) timepoints. Data points represent individual animals, with the line designating
881 the median. Dotted black line indicates the mean preimmune response + 2 standard deviations.
882 *p<0.05, Kruskal-Wallis + *post hoc* Mann-Whitney U test.

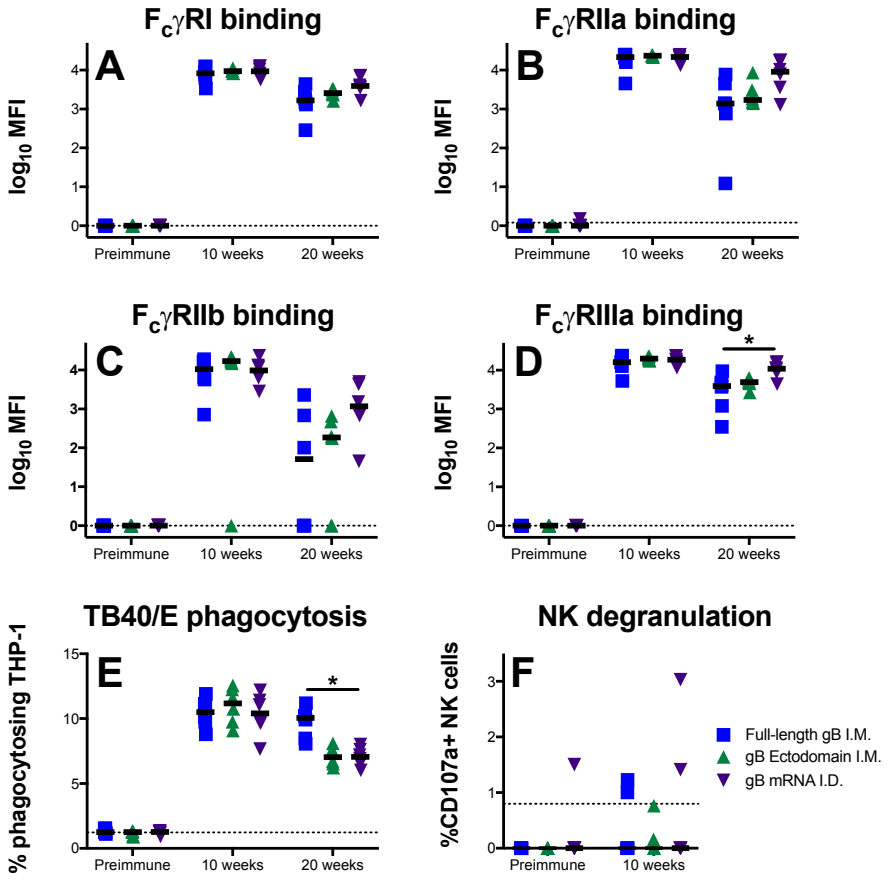

Figure 5. gB mRNA-LNP vaccination elicits long-lived gB-specific IgG-F$_c\gamma$ receptor engagement, though reduced durability of virion phagocytosis response. Vaccine-elicited IgG engagement of FcγRI (A), FcγRIIa (B), FcγRIIb (C), and FcγRIIIa (D) was assessed by BAMA. Phagocytosis of fluorophore-coupled whole HCMV (TB40/E) virions was measured by flow cytometry (E). Upregulation of CD107a on the surface of NK cells in the presence of HCMV-infected cells was assessed by flow cytometry as an approximation of ADCC-activity (F). Full-length gB vaccinees are shown in blue, gB ectodomain in green, and gB mRNA-LNP in purple. Antibody responses were assessed for preimmune, 10 week (post boost 3, peak immunogenicity), and 20 week (necropsy) timepoints. Data points represent individual animals, with the line designating the median. Dotted black line indicates the mean preimmune response + 2 standard deviations. *p<0.05, Kruskal-Wallis + *post hoc* Mann-Whitney U test.

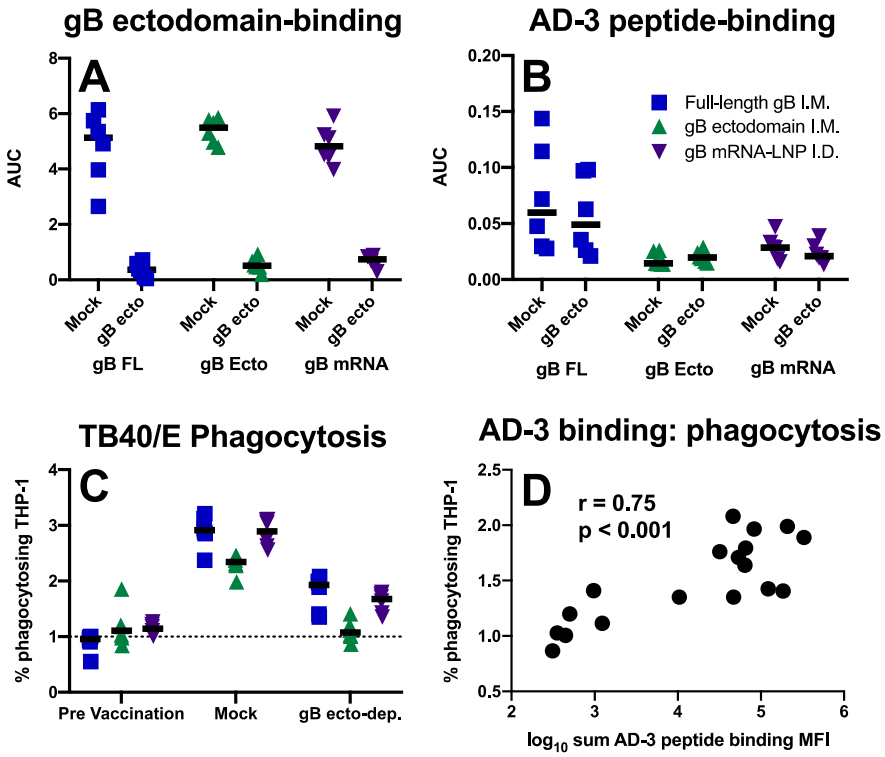

Figure 6. Phagocytosis-mediating antibodies directed against gB AD-3. Binding antibodies targeting gB ectodomain are not detectable in gB ectodomain-depleted sera (A), though antibodies targeting an immunodominant linear peptide within the AD-3 region (QDKGQKPNLLDRLRH) persist (B). 'Mock' = mock depleted sera using HIV-1 gp120, 'gB ecto' = gB ectodomain depleted sera. (C) Phagocytosis of whole HCMV (TB40/E) virions remained measurable by flow cytometry for samples depleted of ectodomain-targeting antibodies (i.e. with AD-3-specific antibodies remaining). (D) Spearman correlation of AD-3 peptide binding IgG magnitude with phagocytosis activity mediated by gB ectodomain-depleted serum antibodies. Full-length gB vaccinees are shown in blue, gB ectodomain in green, and gB mRNA-LNP in purple. Data points represent individual animals, with the line designating the median. Dotted black line indicates the mean preimmune response + 2 standard deviations.

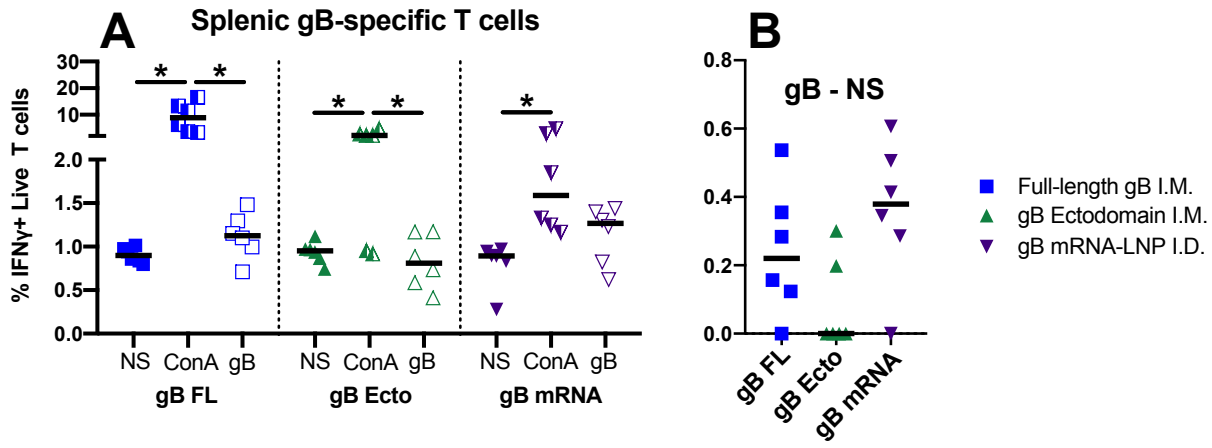

908

909 **Figure 7. Full-length gB and gB mRNA-LNP vaccines elicit antigen-specific T cells in**
910 **spleen of majority of vaccinees.** (A) Splenic cells were either not stimulated (NS), incubated
911 with Concanavalin A (ConA), or with a pool of gB peptides (gB), then stained for Ken-5 (rabbit
912 pan T cell marker) and IFNγ . The percentage of live T cells that stained positive for IFNγ are
913 plotted. (B) For each animal, the difference between the percentage of gB-stimulated and
914 unstimulated cells is plotted. Full-length gB vaccinees are shown in blue, gB ectodomain in green,
915 and gB mRNA-LNP in purple. Data points represent individual animals, with the line designating
916 the median. *p<0.05, Friedman test + *post hoc* Wilcoxon matched pairs signed-rank test.

917 **Tables:**

918

919 **Table 1. Summary of vaccine-elicited immune responses at week 20.**

Category	Median response magnitude	gB FL	gB ecto	gB mRNA
gB Binding	gB FL binding (log_{10} MFI)	2.85	3.37	**3.53***
	gB ecto binding MFI (log_{10} MFI)	2.77	3.19	**3.34***
	Cell-assoc. gB binding (% cells)	18.81	18.58	**29.05***
	RAI (gB FL target)	**0.93**	0.90	0.78
Peptide binding⁺	Total binding sum (log_{10} MFI)	**5.25**	4.74	5.04
	AD-3 binding sum (log_{10} MFI)	**5.12**	2.27	4.77
	# peptides bound (>100 MFI)	44.5	28.5	**85***
Neut. Epitope Binding and Neutralization	Domain I binding (log_{10} MFI)	2.76	3.37	**3.44***
	Domain I+II binding (log_{10} MFI)	2.96	**3.49**	3.03
	AD-1 binding (log_{10} MFI)	NMR†	NMR	NMR
	AD-2 binding (log_{10} MFI)	NMR	NMR	NMR
	AD169r Fibro Neut +C (log_{10} ID_{50})	1.69	1.79	**2.08**
	AD169 Epi Neut +C (log_{10} ID_{50})	1.91	1.83	**2.29**
$F_c\gamma$ receptor binding and function	FcγRI binding (log_{10} MFI)	3.22	3.41	**3.59**
	FcγRIIa binding (log_{10} MFI)	3.14	3.24	**3.29**
	FcγRIIb binding (log_{10} MFI)	1.71	2.27	**3.07**
	FcγRIIIa binding (log_{10} MFI)	3.59	3.69	**4.04***
	TB40/E virion phagocytosis (% cells)	**10.06***	7.04	7.06
	NK degranulation (% cells)	NMR	NMR	NMR
T cells	Splenic gB-specific T cells (BS, % live T)	0.22	NMR	**0.38**

920

921 * p<0.05, Kruskal-Wallis + *post hoc* Mann-Whitney U test (compared to gB FL)

922 ⁺ Peptide binding using week 10 sera

923 † NMR = no measurable response above baseline levels

924

925 **Supporting Information Legends:**

926

927 **Figure S1. Enhanced breadth of gB peptide-binding responses elicited by gB mRNA-LNP**
928 **vaccination.** (A) Sum of linear gB peptide binding IgG magnitude at peak immunogenicity
929 (week 10) to peptides within known antigenic epitopes – AD-1, AD-2 site 1, AD-2 site 2, AD-3,
930 AD-4 (Domain 2), AD-5 (Domain 1), and the furin protease cleavage site. Binding to linear
931 peptides outside these known antigenic regions is denoted 'other'. Full-length gB vaccinees are
932 shown in blue, gB ectodomain in green, and gB mRNA-LNP in purple. Data points represent
933 individual animals, with the line designating the median. *p<0.05, Kruskal-Wallis + posthoc
934 Mann-Whitney U test (B-D).

935

936 **Figure S2. No difference in durability of autologous neutralization between vaccination**
937 **groups.** (A,B) Neutralization of Towne autologous virus in the absence (-C; A) and presence
938 (+C; B) of purified rabbit complement on MRC-5 fibroblast cells. Full-length gB vaccinees are
939 shown in blue, gB ectodomain in green, and gB mRNA-LNP in purple. Data points represent
940 individual animals, with the line designating the median. Dotted black line indicates the mean
941 preimmune response + 2 standard deviations.

942

943 **Figure S3. Rapid induction of gB-specific IgG that engage $F_c\gamma$ receptor following a single**
944 **mRNA vaccine dose.** Vaccine-elicited IgG engagement of FcγRI (A), FcγRIIa (B), FcγRIIb (C),
945 and FcγRIIIa (D) was assessed by BAMA. Antibody responses were assessed for preimmune
946 and 2 week (post boost 1) timepoints. Full-length gB vaccinees are shown in blue, gB ectodomain
947 in green, and gB mRNA-LNP in purple. Data points represent individual animals, with the line
948 designating the median. Dotted black line indicates the mean preimmune response + 2 standard
949 deviations. *p<0.05, Kruskal-Wallis + posthoc Mann-Whitney U test.

950 **Figure S4. Example flow cytometry gating scheme for rabbit splenic T cells.** Spleen cells
951 shown from ConA-stimulated, full-length gB I.M. vaccinated rabbit. (A) Cells were selected using
952 forward and side scatter. (B) Live rabbit T cells were identified using AQUA live/dead stain
953 (Invitrogen) as well as Ken-5 (pan-T cell marker) specific antibody (AF647). (C) IFNγ+ T cell
954 subpopulation identified by intracellular cytokine staining (AF488).

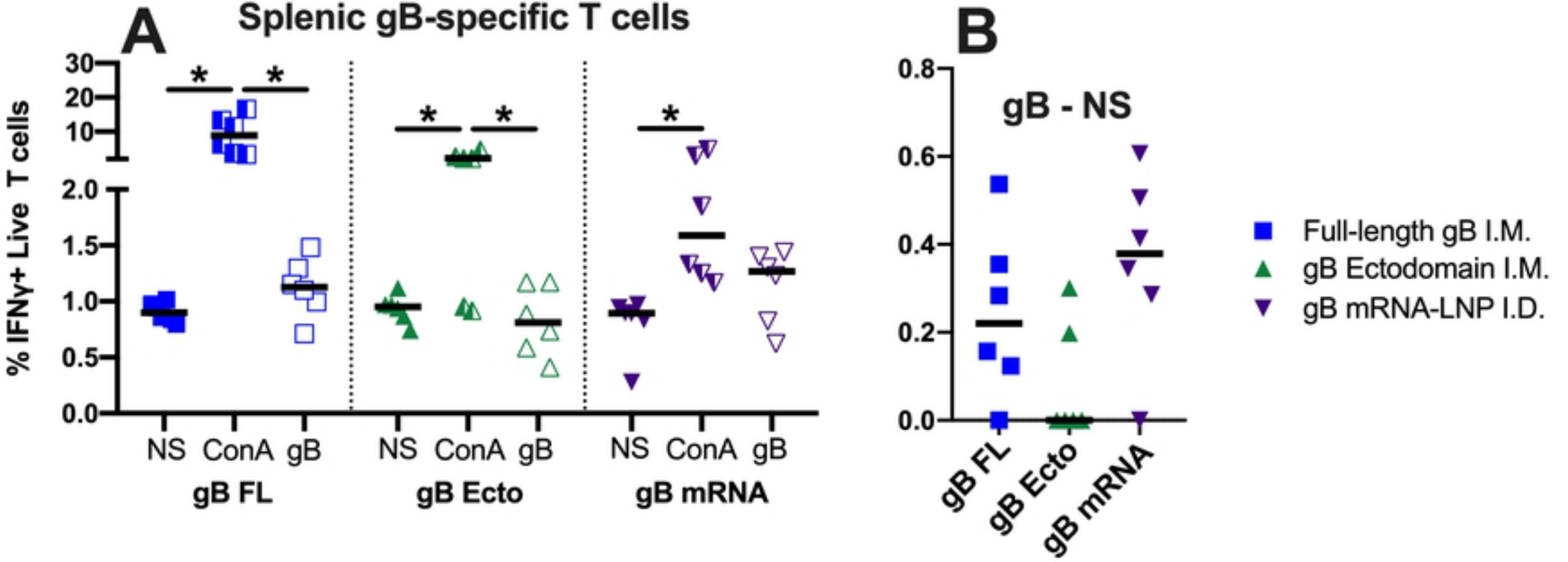
A
Splenic gB-specific T cells
% IFNγ+ Live T cells
30
20
10
2.0
1.5
1.0
0.5
0.0
*
*
*
*
*
NS ConA gB
gB FL
NS ConA gB
gB Ecto
NS ConA gB
gB mRNA
B
gB - NS
0.8
0.6
0.4
0.2
0.0
gB FL
gB Ecto
gB mRNA
Full-length gB I.M.
gB Ectodomain I.M.
gB mRNA-LNP I.D.

Figure 7

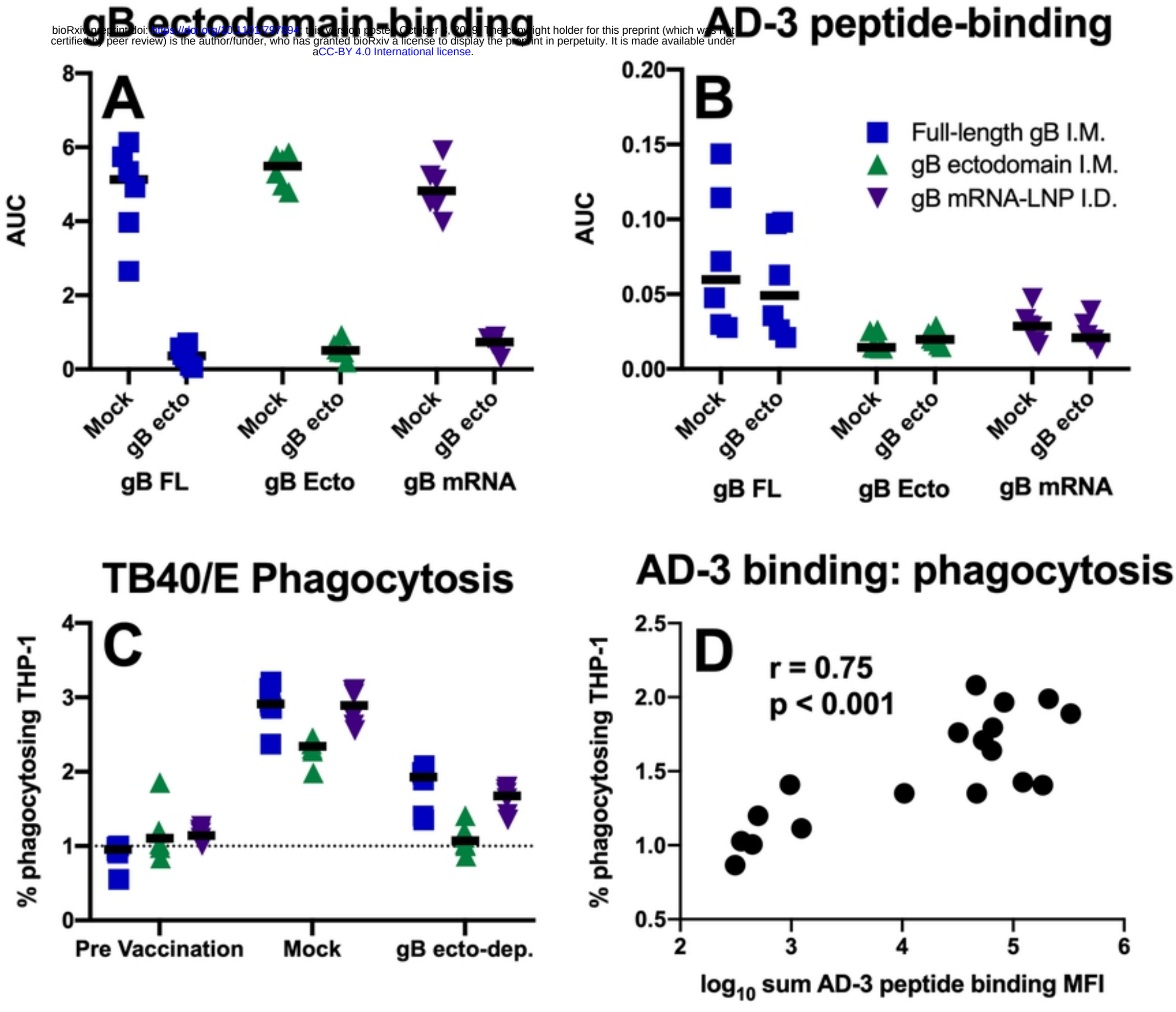

Figure 6

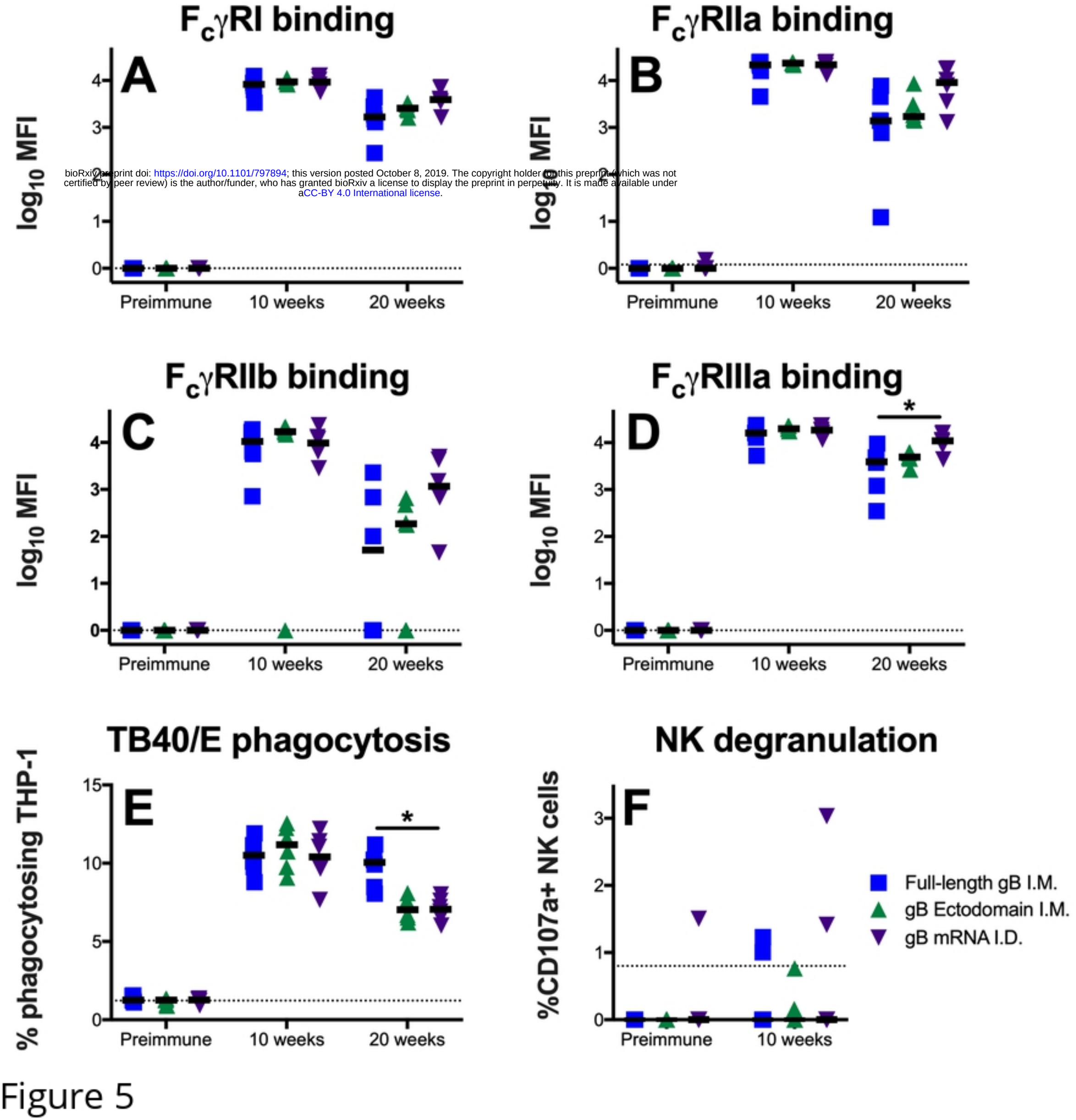

Figure 5

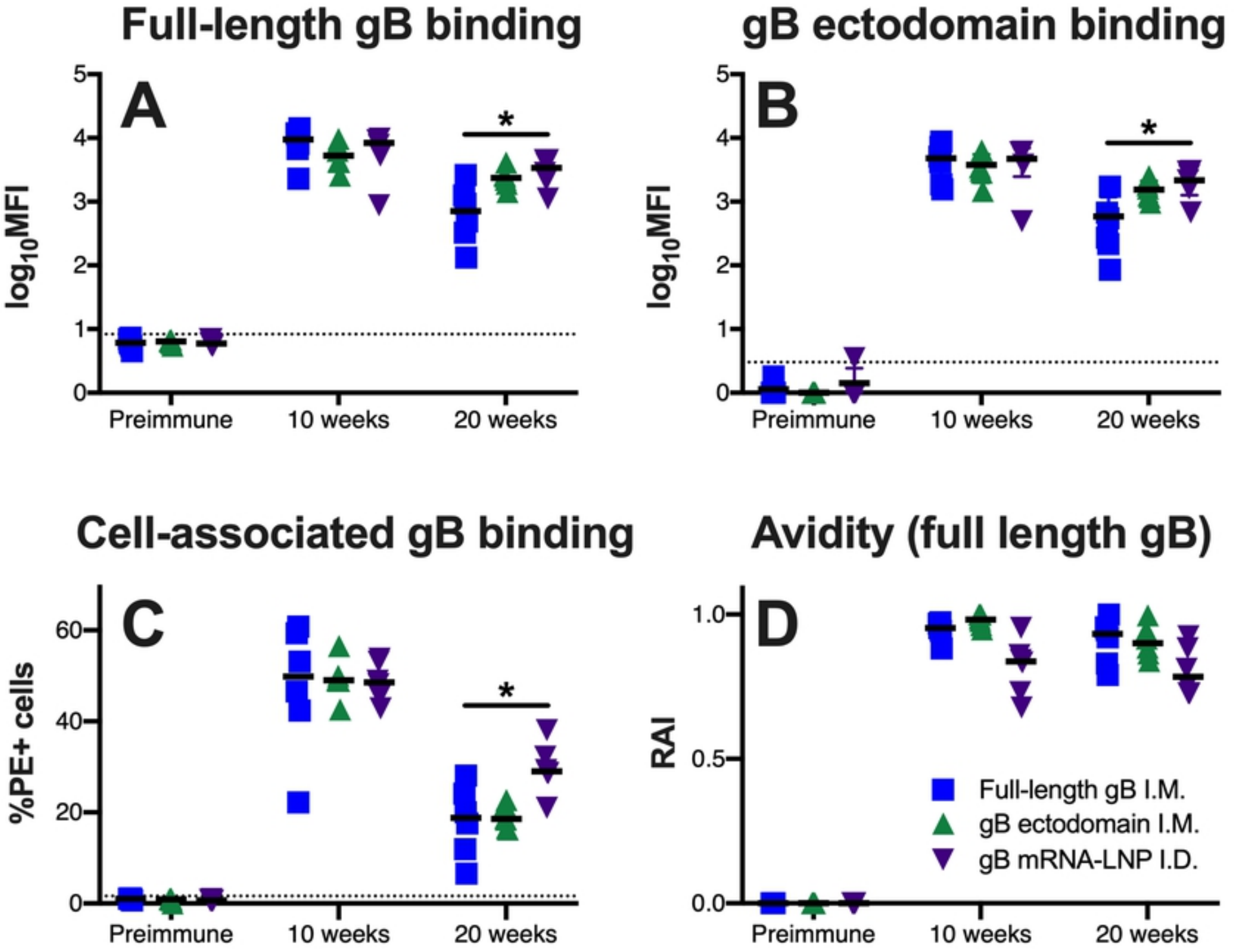
Full-length gB binding
A
log10MFI
0
1
2
3
4
5
*
Preimmune
10 weeks
20 weeks
gB ectodomain binding
B
log10MFI
0
1
2
3
4
5
*
Preimmune
10 weeks
20 weeks
Cell-associated gB binding
C
%PE+ cells
0
20
40
60
*
Preimmune
10 weeks
20 weeks
Avidity (full length gB)
D
RAI
0.0
0.5
1.0
Full-length gB I.M.
gB ectodomain I.M.
gB mRNA-LNP I.D.
Preimmune
10 weeks
20 weeks

Figure 2

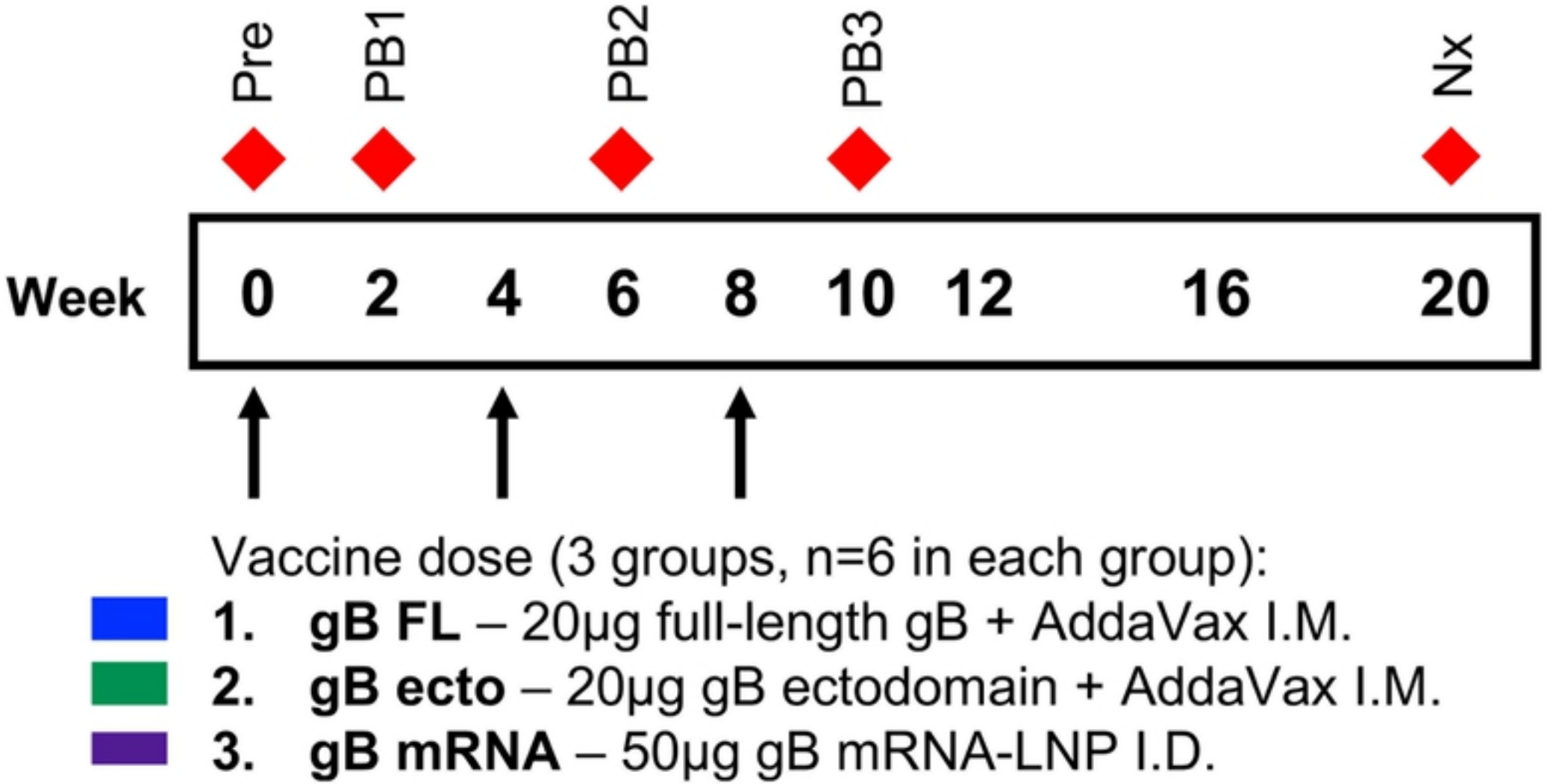
Pre
PB1
PB2
PB3
Nx
Week
0
2
4
6
8
10
12
16
20
Vaccine dose (3 groups, n=6 in each group):
1. gB FL – 20µg full-length gB + AddaVax I.M.
2. gB ecto – 20µg gB ectodomain + AddaVax I.M.
3. gB mRNA – 50µg gB mRNA-LNP I.D.

Figure 1

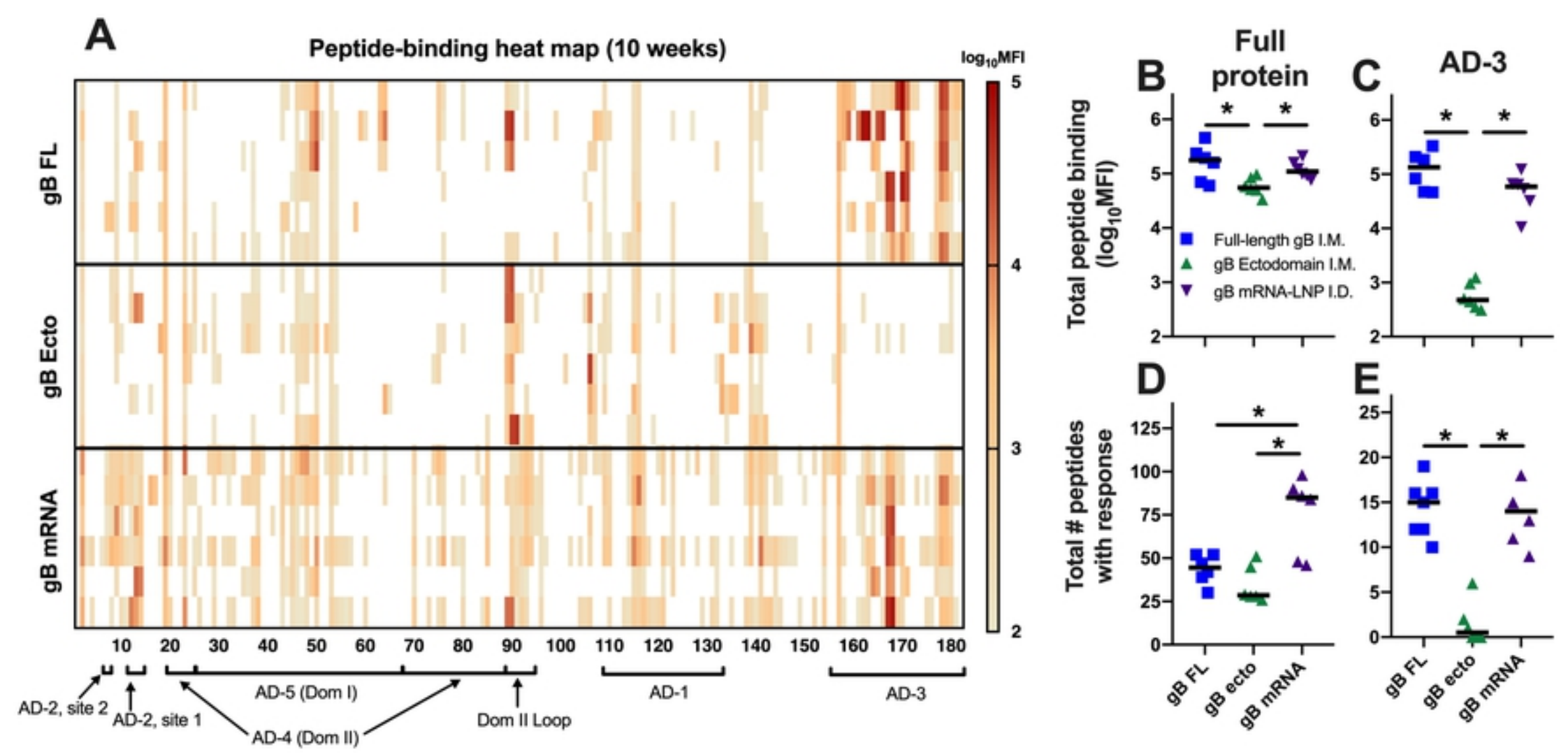
A
Peptide-binding heat map (10 weeks)
log10MFI
5
4
3
2
gB FL
gB Ecto
gB mRNA
10 20 30 40 50 60 70 80 90 100 110 120 130 140 150 160 170 180
AD-2, site 2
AD-2, site 1
AD-5 (Dom I)
AD-4 (Dom II)
Dom II Loop
AD-1
AD-3
B
Full protein
C
AD-3
Total peptide binding (log10MFI)
Full-length gB I.M.
gB Ectodomain I.M.
gB mRNA-LNP I.D.
D
Total # peptides with response
E
gB FL
gB ecto
gB mRNA

Figure 3

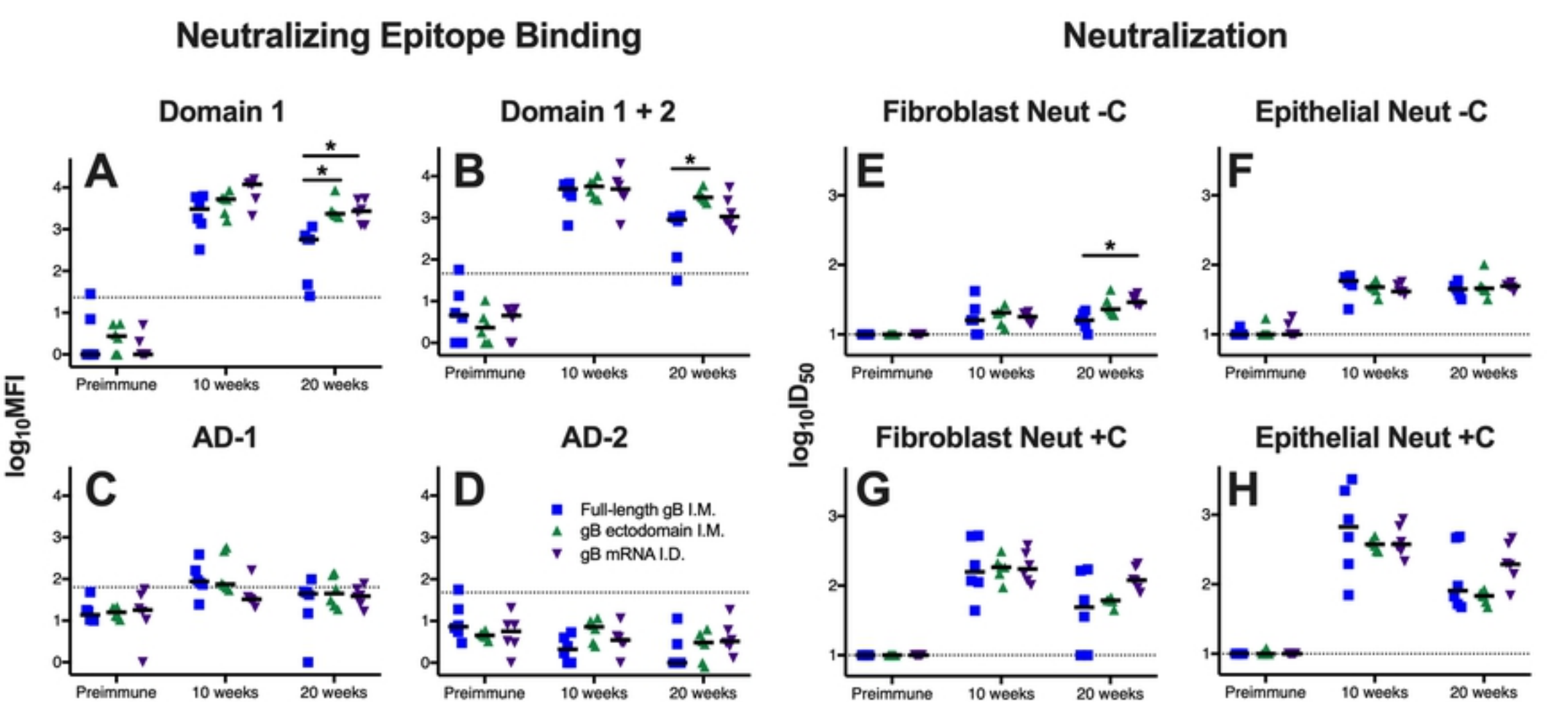
Neutralizing Epitope Binding
Neutralization
Domain 1
Domain 1 + 2
Fibroblast Neut -C
Epithelial Neut -C
A
B
E
F
AD-1
AD-2
Fibroblast Neut +C
Epithelial Neut +C
C
D
G
H
log10MFI
log10ID50
Preimmune
10 weeks
20 weeks
Full-length gB I.M.
gB ectodomain I.M.
gB mRNA I.D.

Figure 4